(2)

Technical Report 1404
December 1990

Detection of Targets in Terrain Clutter by Using Multispectral Infrared Image Processing

L. E. Hoff
J. R. Evans
L. E. Bunney

Approved for public release; distribution is unlimited.

NAVAL OCEAN SYSTEMS CENTER
San Diego, California 92152-5000

J. D. FONTANA, CAPT, USN
Commander

H. R. TALKINGTON, Acting
Technical Director

ADMINISTRATIVE INFORMATION

The work reported here was performed by members of the Processing Applications Branch, Space Systems and Technology Division, Surveillance Department, with funding provided by the Defense Advanced Research Projects Agency (Code AVSTO), 1400 Wilson Boulevard, Arlington, VA 22209.

Released by
D. N. Williams, Head
Processing Applications Branch

Under authority of
F. M. Tirpak, Head (Acting)
Space Systems and
Technology Division

ACKNOWLEDGMENTS

The authors would like to thank Larry Stotts, DARPA, and Ed Winter, Technical Research Associates, who have also been deeply involved in the development of signal-processing algorithms for multispectral imagery. This work was partially funded by the DARPA Multi-Spectral Infrared Camera (MUSIC) program.

SUMMARY

PROBLEM

Investigate a weighted-difference signal-processing algorithm for detecting ground targets by using dual-band IR data.

RESULTS

Three variations of the algorithm were evaluated: (1) simple difference; (2) minimum noise; and (3) maximum SNR. The theoretical performance was compared to measured performance for two scenes collected by the NASA TIMS sensor over a rural area near Adelaide, Australia, and over a wooded area near the Redstone Arsenal. The theoretical and measured results agreed extremely well. For a given correlation coefficient and color ratio, the amount of signal-to-noise ratio gain can be predicted. However, target input SNRs and color ratios can vary considerably. For the targets and scenes evaluated here, the typical gains achieved ranged from a few dB loss (targets without color) to a maximum of approximately 20 dB.

CONTENTS

FIGURES

TABLES

1.0 INTRODUCTION

The detection of small targets in clutter is a problem of critical importance to wide-area surveillance [1]. Stealth technology has made targets more difficult to detect. Targets can also hide in clutter that is either manmade or natural. One technology continuously being investigated for improving small-target detection in clutter is infrared (IR) imagery. Multispectral IR films have been effective for detecting some forms of camouflaged targets and other targets using false coloring [2]. Recently, interest in using multispectral sensor data in signal processing was stimulated by an analysis of such data collected by the NASA Thermal Infrared Multispectral Scanner (TIMS) sensor in Australia during 1985 [3]. These data and their analysis [4] suggested that multispectral processing techniques could greatly improve detection of small, hard-to-find targets.

The work presented here is part of the DARPA Multi-Spectral Infrared Camera (MUSIC) program. Several algorithms have been developed and tested on infrared data [5,6,7].

The objective of this work was to investigate weighted difference, a signal-processing algorithm for detecting ground targets by using dual-band IR data. This algorithm is derived, analyzed, and compared to empirically measured results.

Section 2.0 gives a derivation of the algorithm and its theoretical signal-to-noise ratio (SNR) of input to output. Section 3.0 gives the results of applying the algorithm to two image scenes, and compares the results to the theoretically predicted performance (showing excellent agreement). Numerical details supporting this work have been included in the appendices.

2.0 MULTISPECTRAL PROCESSING CONCEPTS

There are two principles we exploit in our use of multispectral IR imagery. The first is that IR images of natural backgrounds in different long-wave infrared (LWIR) bands tend to be highly correlated. This high degree of correlation allows the data collected in one spectral band to be used to cancel the background clutter in the data collected in another spectral band. The second principle involved is that the LWIR signatures of manmade objects generally do not exhibit the same relationship between bands as do the correlated background signatures. We refer to this difference in target signature between bands as "coloring."

The algorithm for weighted differences is the following: the scene data in one band are multiplied by a constant and subtracted from the scene data in the other spectral band on a pixel-by-pixel basis. The constant is chosen so that the background clutter in the resulting image is minimized. While the background is minimized, the target will leave some residual in the output image because of its coloring between spectral bands. Target coloring and background correlation determine the performance of the weighted-difference algorithm.

The output radiance for each band is the sum of target signal and background clutter. The background clutter is assumed to be made up primarily of natural vegetation or clouds (which are grey bodies), so the clutter will be highly correlated from one band to the next. Sensor noise and "colored," or nongrey, bodies in the image will reduce the correlation coefficient between the two bands. The targets are assumed to be manmade objects and are characterized as selective radiators, which can have a different radiance level, or color, in each band.

The sensor either scans or uses a focal-plane array to collect data in a rectangular image. The data consist of pixels that are modeled as being either target or background clutter. Each pixel records a measure of the received IR radiance for that image cell. The target pixel obscures the background, so these pixels contain only target radiance and no background.

Let the target pixel be given by S_i and clutter pixels be labeled as N_i, where $i = x$ or y for bands x and y, respectively. The target radiance in the bands is given by

$$S_i = e_{si}B(T) \qquad i = x, y \tag{1}$$

and the background radiance is given by

$$N_i = e_{ci}B(T_c) \qquad i = x, y \tag{2}$$

where

T = the target temperature

T_c = the temperature of the background

e_{si}, e_{ci} = the emissivity coefficients for target and clutter

B = Planck's black–body function .

N_i is a random variable because of random variations from pixel to pixel of the emissivity and clutter temperature. Let m_i and v_i be the mean and variance of the clutter for band i. The standard deviation is the square root of the variance and will be denoted as σ_i. The correlation coefficient of the two bands is then given by

$$\rho = \frac{Cov(N_x, N_y)}{\sigma_x \sigma_y} . \tag{3}$$

Figure 1 gives a block diagram for the weighted-difference algorithm. The algorithm multiplies the image from band y by a constant weight, ω, and subtracts it from the image from band x. The objective of the algorithm is to produce an output image that enhances the target signal-to-noise ratio. There are three variants of the algorithm, depending on how the constant, ω, is derived.

Variant 1: Max_SNR

Choose ω to maximize the output SNR.

Variant 2: Min_Noise

Choose ω to minimize the variance of the output image.

Variant 3: Sim_Diff

Choose ω = 1.0.

Define the input pixel signal-to-noise ratio to be

$$psnr(i) = \frac{[Targetpixel(i) - m_i]}{\sigma_i} . \tag{4}$$

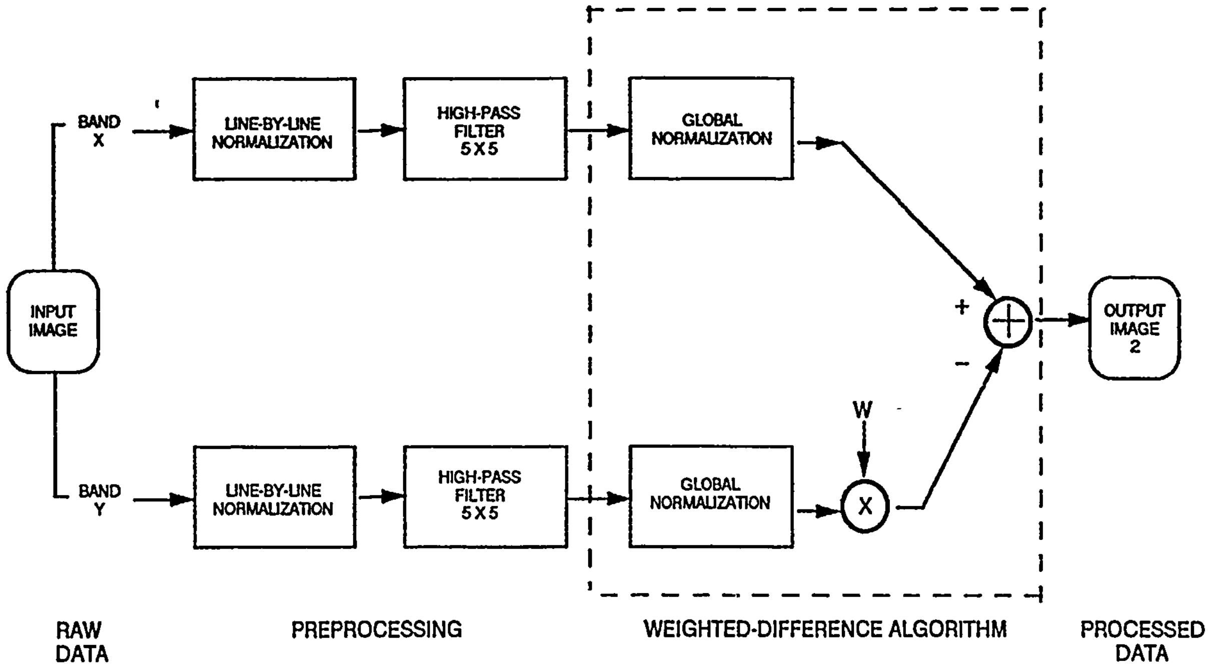

Figure 1. Processing flow for weighted-difference algorithm.

The signal-to-noise ratio is measured in dB, given by the following

$$\mathrm{SNR}_{in}\ (\mathrm{dB}) = 10\log[psnr(i)]^2 \tag{5}$$

where i denotes the band.

Let V be the output variance when only clutter is present; then the output signal-to-noise ratio that is to be optimized is SNR_{out}, where

$$\mathrm{SNR}_{out} = \frac{(S_x - \omega S_y)^2}{V} . \tag{6}$$

The output variance can be shown to be a function of the input statistics as

$$V = \sigma_x^2 - 2\omega\rho\sigma_x\sigma_y + \omega^2\sigma_y^2 . \tag{7}$$

The three variants of the weighted-difference algorithm can be derived from the above equation. However, the derivation is simpler and easier to implement if each channel is normalized to have mean equal to zero and variance equal to one. The output SNR becomes

$$\mathrm{SNR}_{out} = \frac{(S_{nx} - \omega S_{ny})^2}{(1 - 2\omega\rho + \omega^2)} \tag{8}$$

where

$$S_{ni} = \frac{(S_i - m_i)}{\sigma_i} \qquad i = x, y \,. \tag{9}$$

The weight for variant 1, $\omega_{\text{max\_SNR}}$, can be determined by taking the derivative of the SNR_{out} with respect to ω and setting it to zero to find the critical points. There are two critical values (see appendix B). The one that maximizes the SNR_{out} is variant 1:

$$\omega_{\text{max\_SNR}} = \frac{\rho - c}{1 - \rho c} \tag{10}$$

where c is defined as the ratio of the pixel signal-to-noise ratios,

$$c = \frac{psnr_{\min}}{psnr_{\max}} , \qquad -1 \le c \le 1 \,. \tag{11}$$

When $c = \rho$ the weight is zero. This can be interpreted to mean that, for the Max_SNR algorithm, the two bands should not be combined and the best output image when $\rho = c$ is the input image from band x. Note also that, when $c = 1/\rho$, the weight is infinity. This can similarly be interpreted to mean that, for the Max_SNR algorithm, the two bands should not be combined and the best output image when $c = 1/\rho$ is the input image from band y. To avoid potentially large values of ω, the input bands were arranged so that band x was always the band with the largest *psnr*.

To implement the Max_SNR algorithm, we need to know the color ratio of the target pixels. For selective radiators, this ratio would not be known ahead of time. For the calculations here, we knew where the target pixels were and measured the color ratio from the actual data, which is not a very practical algorithm implementation. One could come up with some clever scheme to predict or estimate the color ratio, but it will be shown that the performance of the Max_SNR is not sufficiently better than the other algorithms to warrant the effort. The other algorithms do not require this information, and are much simpler to implement. The Max_SNR algorithm serves as an upper bound to the performance obtainable from a weighted-difference algorithm.

The weight for variant 2, $\omega_{\text{min\_noise}}$, can be determined by taking the derivative of that quantity and finding the value of ω that minimizes the denominator. There is only one solution for ω in this case which is

$$\omega_{\text{min\_noise}} = \rho \,. \tag{12}$$

The Min_Diff algorithm does not require knowledge of the target color. However, the algorithm has a similar problem to Max_SNR in that it must know which band has the largest input SNR. If this is unknown, the algorithm must be performed twice, once for x hypothesized as the largest and once for y. Both outputs must be threshold tested for detections. The penalties for not knowing which channel has the largest input SNR are increased computation and either a higher false-alarm rate or a higher threshold value—which will reduce the number of detections.

The weight for the simple difference variant is simply

$$\omega_{\text{sim\_diff}} = 1.0 \,. \tag{13}$$

The output SNR_{out} for each variant can be found by substituting the appropriate solutions for ω back into equation (8). Table 1 summarizes the three variants of the weighted-difference algorithm.

Table 1. Variants of the weighted-difference algorithm.

Case1 : Max_SNR

$$\omega = \frac{\rho - c}{1 - \rho c}$$

$$\mathrm{SNR} = \frac{S_1^2}{\sigma_1^2} \cdot \frac{(1 - \omega c)^2}{1 - 2\omega\rho + \omega^2}$$

Case 2: Min_Noise

$$\omega = \rho$$

$$\mathrm{SNR} = \frac{S_1^2}{\sigma_1^2} \cdot \frac{(1 - \rho c)^2}{1 - \rho^2}$$

Case 3: Sim_Diff

$$\omega = 1.0$$

$$\mathrm{SNR} = \frac{S_1^2}{\sigma_1^2} \cdot \frac{(1 - c)^2}{2(1 - \rho)}$$

Figure 2 is a plot of the theoretical output SNR for a band-to-band correlation coefficient of $\rho = 0.9$. The dB gain is very dependent on the color ratio. When the color ratio is 1, there is no color to the target. When the color ratio is negative, the target contrasts in the two bands have opposite signs; i.e., the target in one band is above its mean level and the target in the other band is below its mean level. The gain from these multispectral algorithms is greatest for negative color ratios. This is an important point since, for this to occur, the target must be near zero contrast and difficult to detect by spatial processing alone.

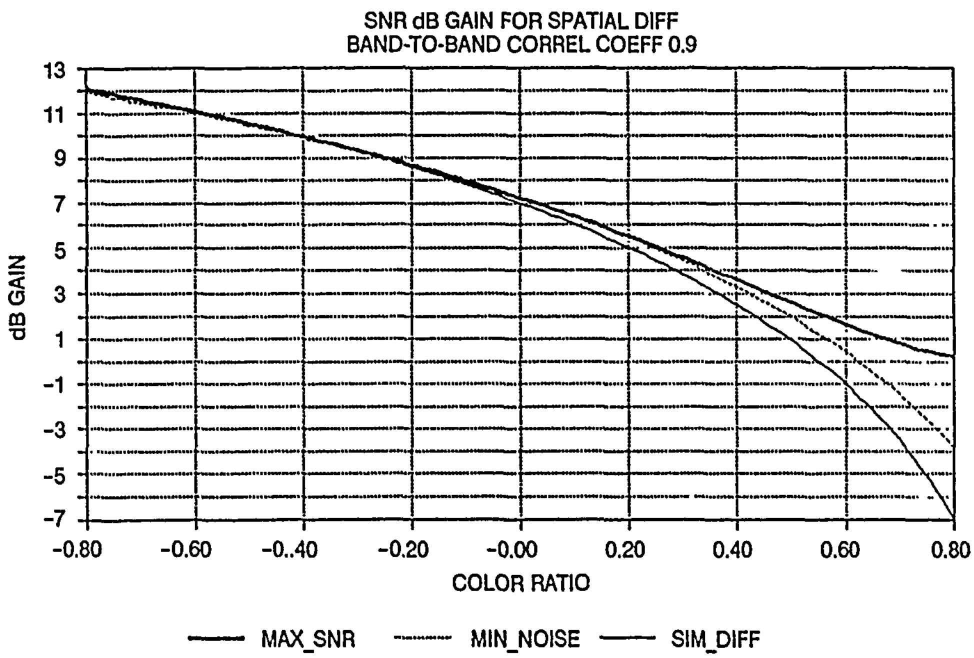

Figure 2. Weighted-difference algorithm variants for a background band-to-band correlation of 0.9.

Figure 3 shows three cases of interest. The first shows the radiance levels when the target appears hot compared to the background mean level. In this case, the input SNRs are positive and large (for this simple argument, the variance of the background about the mean level is not shown). The SNRs in the two channels are different only by the factor of the emissivity. Thus the ratio, *c*, will be positive and close to 1. In case 2, the input signal-to-noise ratios are small because they are close to the background mean level. Here the ratio of the SNRs can be magnified, depending on the mean level. The ratio of the SNRs could be large and possibly negative. This condition results in large SNR gain. In case 3, the target appears cold compared to the background. If the SNRs are large (but negative), the ratio again will be positive and close to 1. This results in a small gain.

Figure 4 is a theoretically derived curve comparing the output SNR from a spatial-differenced system with the best input SNR. The model parameters were arbitrarily chosen, but the figure illustrates the behavior of the differenced algorithm. It tends to provide gain when the input SNR is small. This characteristic "fills in" the SNR output curve when the input SNR is small.

3.0 COMPARISON OF THEORETICAL AND EXPERIMENTAL RESULTS

In this section, the theoretical performance is compared to measured performance for two multispectral infrared scenes collected by the NASA TIMS sensor. The first scene was collected over a rural area near Adelaide, Australia, and the second scene was collected over a mixed wooded and open-field area near the Redstone Arsenal in Huntsville, Alabama. The TIMS sensor has six channels between 8 and 12 μm; however, only two were used for weighted-difference application. Scenes were selected that were 512 × 512 and 256 × 256 pixels in dimension for the Adelaide scene and 256 × 256 for the Redstone scene. Each scene contains a number of manmade objects in a cluttered background that served as targets. There were 52 objects (houses, farm buildings, watertanks, etc.) in the Adelaide 512 × 512 scene that were declared targets and used to evaluate the dB gains as a function of the input SNR and detection statistics. There were 14 declared targets in the Adelaide 256 × 256 image that were used to evaluate SNR statistics. The analysis was repeated on the Redstone scene; however, this time military tanks (M60 and M48) were located in the scene as part of the experiment. The Redstone scene was used to confirm the results achieved by using the Adelaide data.

3.1 EXPERIMENTAL RESULTS FROM THE ADELAIDE SCENE

The TIMS Australian data set was acquired as part of a joint U.S and Australian measurements program conducted in the fall of 1985 over several regions of Australia. The data set was obtained from a C-130 aircraft at a variety of altitudes. A review of the data taken during this particular acquisition found a rural natural background area in the hills east of Adelaide. A subsection of this area containing structures was selected for spectral processing [6].

Figure 5 is a grey-level image of the Adelaide 256 × 256 scene. The C-130 flew at a low altitude, which resulted in a ground resolution of 2.5-meter pixels. Channels 1 and 5 were selected for processing because they gave the best target color ratios and band-to-band clutter correlation. Figure 6 shows the output scene from the weighted-difference algorithm. The minimum noise variant with full preprocessing (i.e., line-by-line normalization and high-pass filtering) was used. Note that the output targets can have positive (bright) or negative (dark) contrast. Details of the numeric results are given in appendix A.

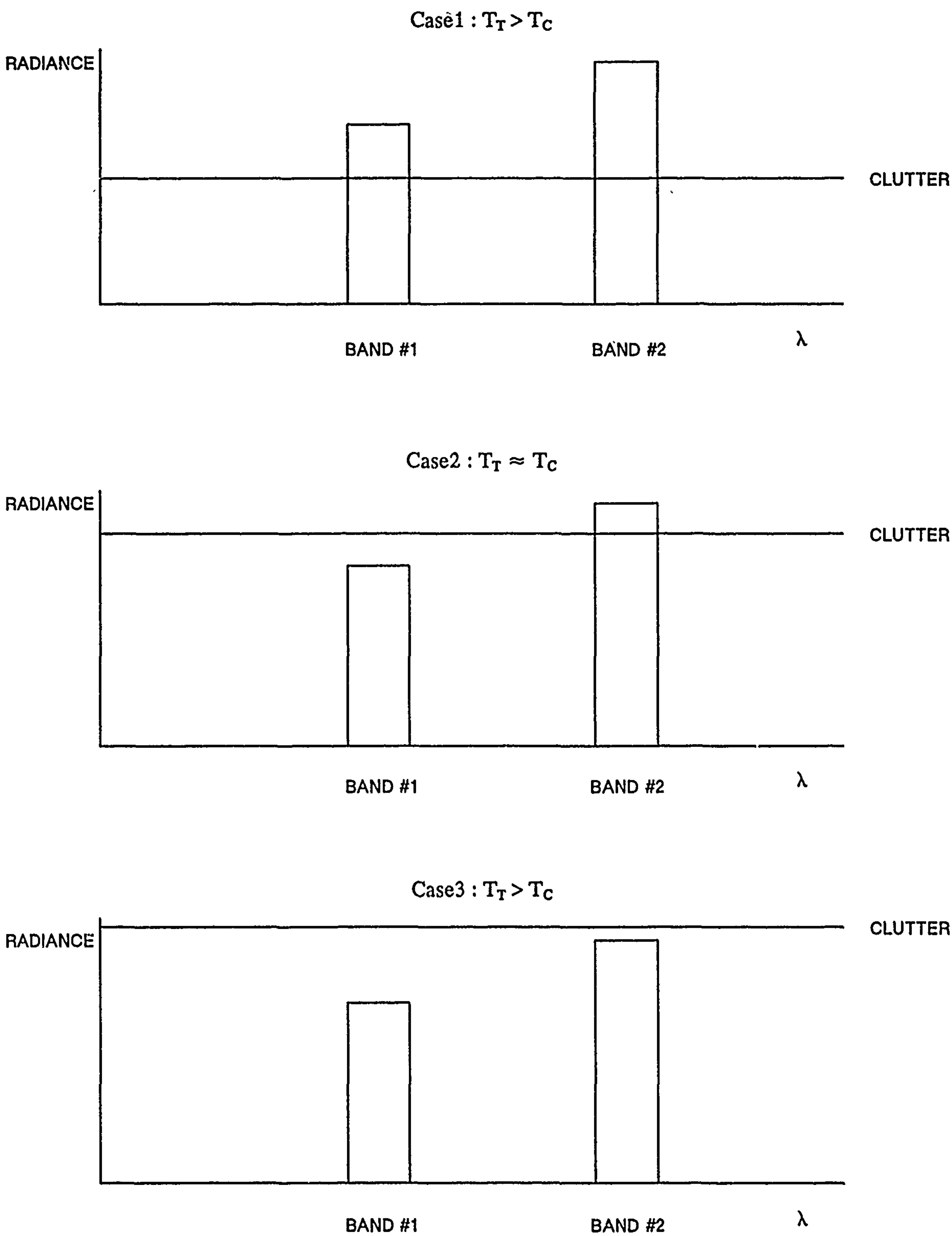

Figure 3. Three cases of relative target and background temperatures.

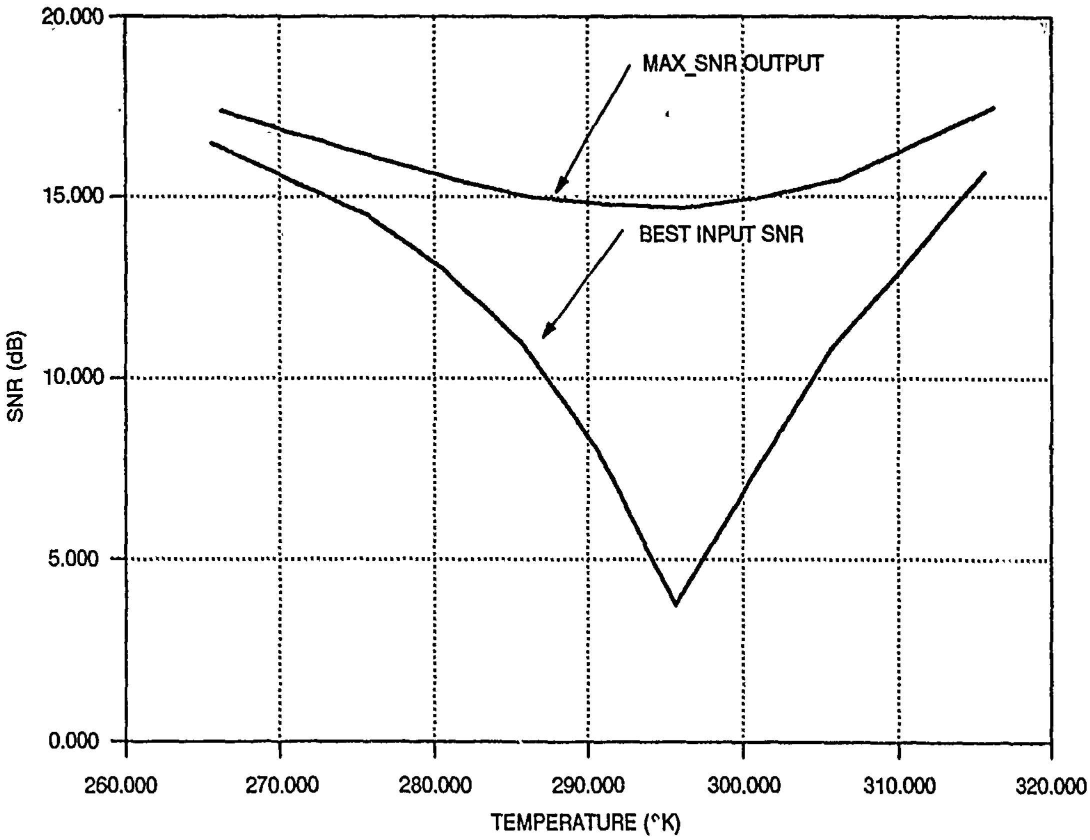

Band #1 = 8.2-8.6μm

Band #2 = 9.4-10.2μm

Clutter at 290°K

Rad sigma (σ) = 8% of B(290)

$$psnr(i) = \frac{[Targetpixel(i) - m_i]}{\sigma_i}$$

SNR (dB) = 10 log[$psnr(i)$]^2

Let e_{s1}= 0.80, effective emissivity of target in band 1

Let e_{s2}= 0.99, effective emissivity of target in band 2

Assume e_{ci} = 1.0, where e_c is emissivity of background

Band-to-band correlation coefficient ρ= 0.9.

Figure 4. Channel radiance versus temperature.

A rural area near Adelaide, South Australia, consisting of scattered trees, a forested region, rolling hills, and manmade structures. The image has 256 $\times$ 256 pixels that have 2.5-meter ground resolution Channels 1 and 5 were used for multispectral processing.

Figure 5. Adelaide scene.

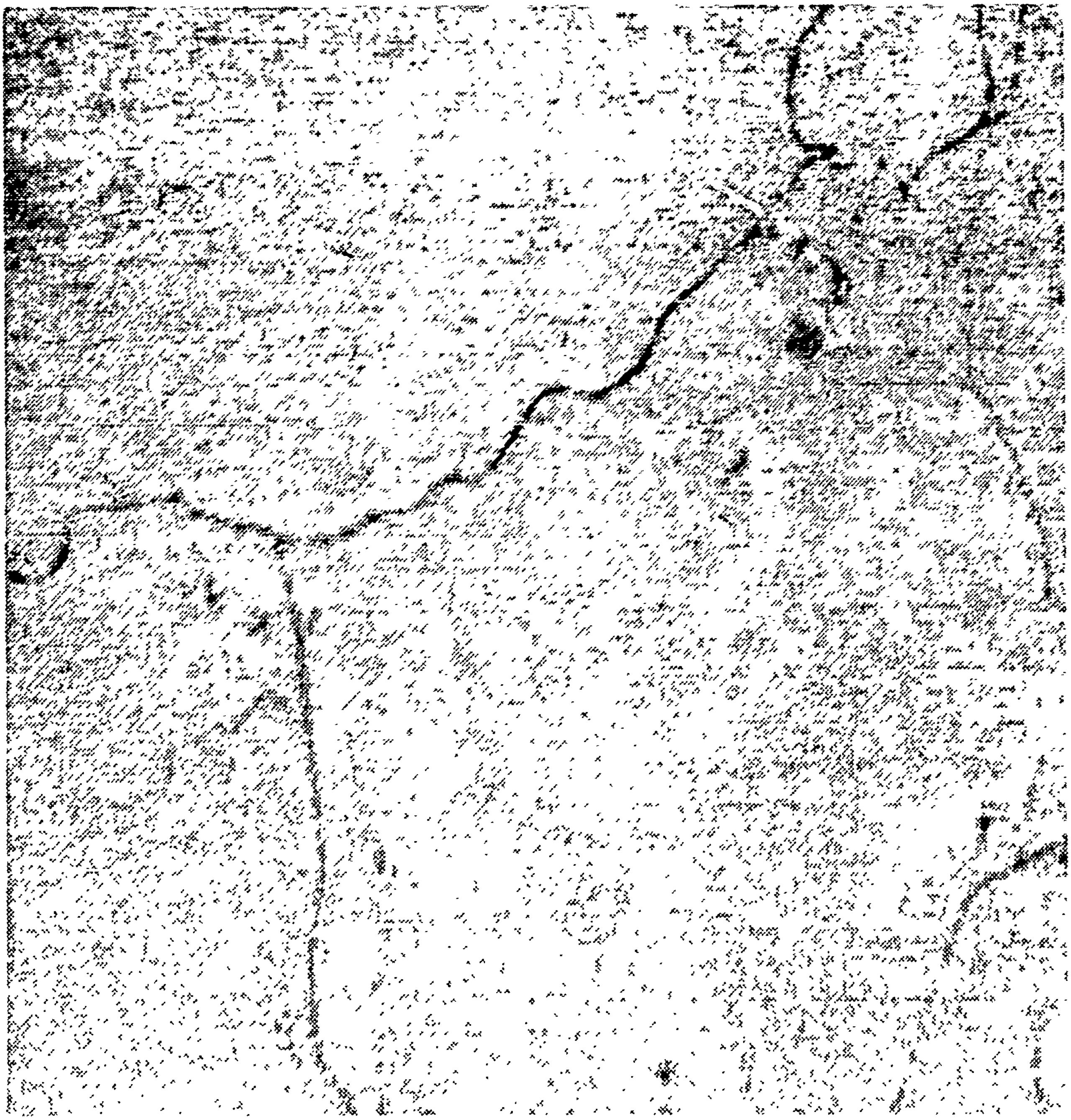

Minimum noise variant used with line-by-line normalization and high-pass filter preprocessing
Fourteen output targets are single pixels that are either bright or dark

Figure 6. Adelaide—weighted-difference output.

The results of processing the Adelaide 256 × 256 data are compared to the theoretical output signal-to-noise ratio in figures 7a and 7b. First the multispectral images were processed without preprocessing and the results are shown in figure 7a. The signal-to-noise gain, measured in dB, is plotted as a function of the color ratio. The correlation coefficient for the Adelaide scene was 0.9929. There are three curves on the graph that are the theoretically predicted gain for the three variants of the weighted-difference algorithm. The symbols represent measured gain on targets in the Adelaide scene. There is excellent agreement between the theory and measured results.

Similarly, figure 7B presents the same information, except that in this case the data set was preprocessed as shown in figure 1. The signal-to-noise ratio gain is measured from the input to the output of the weighted difference algorithm, and does not include the SNR gain or loss caused by the preprocessing. In general, the weighted difference gains are much lower with preprocessing than without preprocessing, as can be seen by comparing the results to the example in figure 7. The reason for the drop in gain is that the preprocessing has reduced both the band-to-band correlation and the color ratio. However, the preprocessing also provides gain, so the overall effect is a net improvement over no preprocessing. The output signal-to-noise ratio level for preprocessing and no preprocessing are summarized in tables A4 through A6 of appendix A. With a few exceptions, the combination of preprocessing and weighted difference improved the overall output signal-to-noise ratio by 1 or 2 dB. The significant conclusion from figures 7a and 7b is that the SNR performance of the weighted-difference algorithm can be predicted.

Figure 8 shows the output signal-to-noise ratio plotted versus the input average pixel-to-noise ratio. The pixel signal-to-noise ratio is given by equation (4). The average *psnr* is a function of the difference between the target and the mean background temperatures. Using measured data from the Adelaide 512 × 512 scene (see appendix C), figure 8 compares the best input signal-to-noise ratio to the min_noise (without preprocessing) output SNR. The data have the same trend as the theoretical data shown in figure 4. The data are not smooth because the targets do not have the same emissivity, which causes the gain to vary for targets even at the same temperature. Regardless, the gain appears to be maximum near zero, as in figure 4, and shows the characteristic of the weighted-difference algorithm to "fill in" the output SNR when the target is small because of marginal target temperature difference from the background.

The detection statistics for the 52 targets in the Adelaide 512 × 512 scene were computed for 10^{-3} and 10^{-4} false-alarm rates, and the results are summarized in table 2. Details of the numeric results are provided in appendix C. The threshold for the false-alarm rates was computed from the data after the 52 targets were omitted from the 512 × 512 image. As shown in figure 8, the performance improvement of the weighted-difference algorithm depends on the relative target temperature to the average background temperature as well as the target emissivity. Thus the number of detections in table 2 depend on the statistical distribution of the target temperature and emissivity provided in the Adelaide scene.

Table 2. Detection statistics for 52 targets in the Adelaide scene.

Processing Algorithm (Bands 1 and 5)	Detections at CFAR 10^{-3}	10^{-4}
No Preprocessing		
Band 5—Raw Input	28	20
Simple Difference	44	18
Minimum Noise	45	18
Preprocessed		
Band 5	34	19
Simple Difference	47	23
Minimum Noise	47	19.

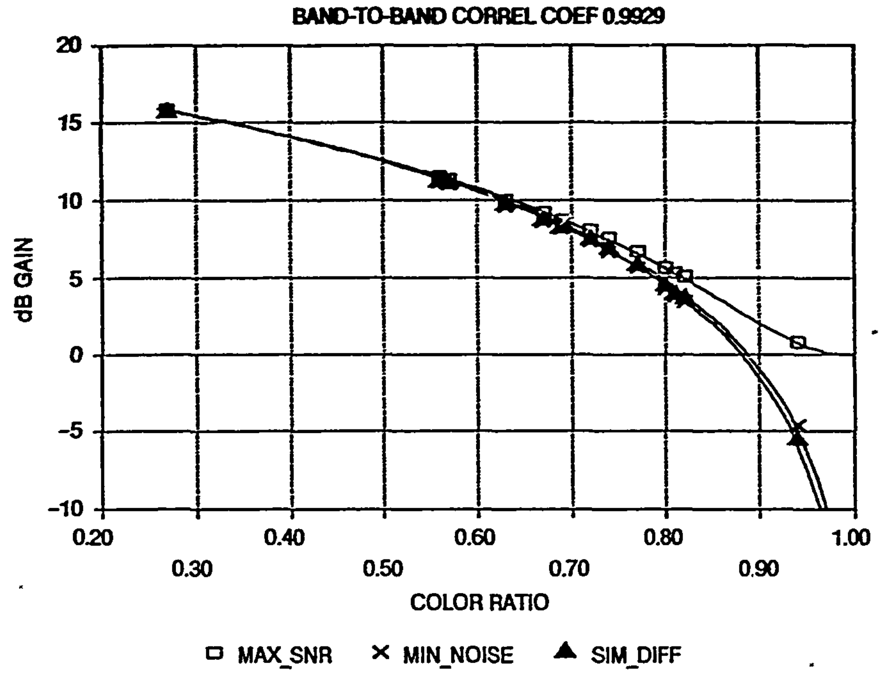

(a)

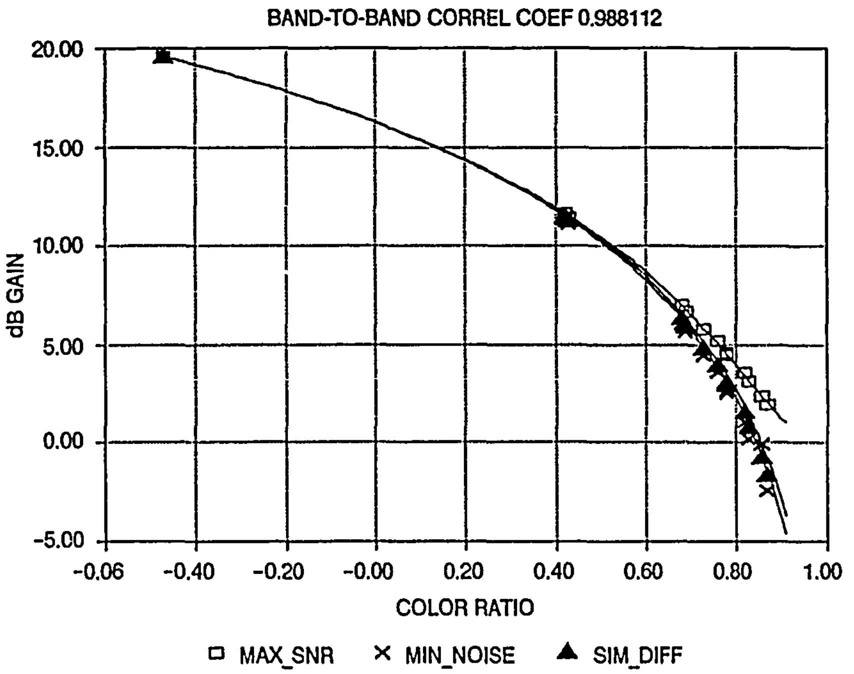

(b)

Actual data points from the Adelaide 256 × 256 scene plotted on the theoretical curves for the three variants of the weighted-difference algorithm.

Figure 7a-b. dB gain as a function of color ratio.

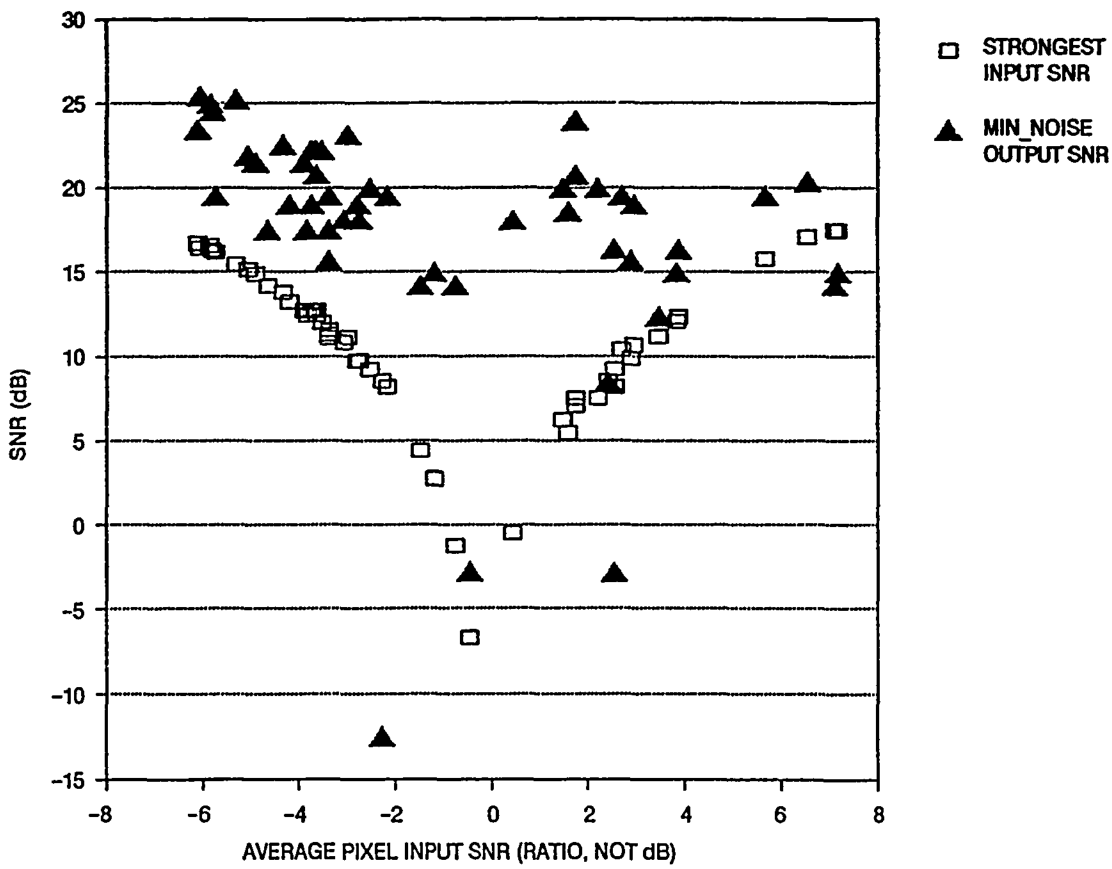

Actual data points from the Adelaide 512 X 512 scene. Compare with figure 4.

Figure 8. dB gain as a function of input SNR.

Without any processing, 28 of the 52 targets could be detected at a 10^{-3} false-alarm rate. With full preprocessing and the minimum-noise-difference algorithm, this number was increased to 47. The detection rate improvement from 54% to 90% is a very significant result.

3.2 EXPERIMENTAL RESULTS FROM THE REDSTONE SCENE

The Redstone experiment was performed on 9 March, 1989, at Redstone Arsenal, Alabama, using the TIMS sensor. A Lear Jet was flown during two time periods, 0800 to 0900 and 1100 to 1200 h. A data set was taken during each of these flights at three different altitudes, resulting in a resolution of 2.5, 5, and 10 meters. The weather was clear, with a slight breeze and moderate haze that burned off during the morning. The air temperature increased from 39 to 51°F.

The experimental setup was located at Redstone Arsenal's Test Area No. 3, which consists of slightly rolling hills with a grass-covered stretch of land surrounded by loblolly pines and deciduous trees. The grass was disturbed as a result of tank movements in the field. Three tanks were set up as targets, and nearby temporary buildings and a concrete pad located to the south of the tanks were used as targets of opportunity. Tank A, an M48, was located on the edge of the field with trees just to the west. Tank B, an M60, was under the trees on a dirt road covered with pine needles. The trees provided about a 50% canopy over the tank. Tank C, another M48, was located in the open field. The ground was less disturbed around tank C than tank A. Tank B, the tank under the trees, was not observed with the infrared sensor or high-resolution photography.

Both tank A and tank C were detected in the 2.5-m data by means of several algorithms in both the morning and noon scenes. Tank C, the open-area tank, was also detected in the lower-resolution data. In this section, we will concentrate on the detections made during the early-morning 2.5-m scene, with particular emphasis on the tree-line tank A. A gray-level image of the scene showing the tank locations is given in figure 9.

Bands 1 and 4 of the TIMS data were spectrally processed and the detailed numeric results are given in appendix D. Bands 1 and 4 were chosen since they show spectral color. The results for a 32×32 image centered on the tree line of tank A are shown in figure 10. The tree-line tank, not discernible in the input data in figure 10A, can be seen easily in figure 10B.

The location of a target detection relative to false alarms is an important indication of algorithm performance, since a constant false-alarm rate system would need to suppress false alarms to a specified level. The cumulative distributions for the unprocessed input and processed data are shown in figures 11a and 11b. Tank A and C pixels were removed before calculating the distributions. The curves can be used to estimate the false-alarm rate that would result for a given threshold decision level. For unprocessed input data, the false-alarm rate would have to be 2×10^{-1} before the target could be detected. After processing, a more reasonable false-alarm rate of only 7×10^{-5} would have to be tolerated. (Recall that, if the strongest input channel were not known *a priori*, a double-sided threshold would be required). The double-sided threshold could double the number of false alarms to 1.4×10^{-4}, which is still a reasonable value. The false alarms at thresholds greater than tank A were caused by man-made structures (concrete pad, buildings, vehicles) in the scene, which were also colored. These man-made objects can be considered as targets in the context of a natural scene.

The various colored, manmade objects in the scene can be used to verify the theory presented earlier. The output depends on the amount of target coloring [see equations (8) and (10)]. Each of these objects has a different color ratio. These objects were identified by means of site visits and aerial photography. The objects investigated included two structures, two pixels on tank C, tank A, and a rectangular concrete pad.

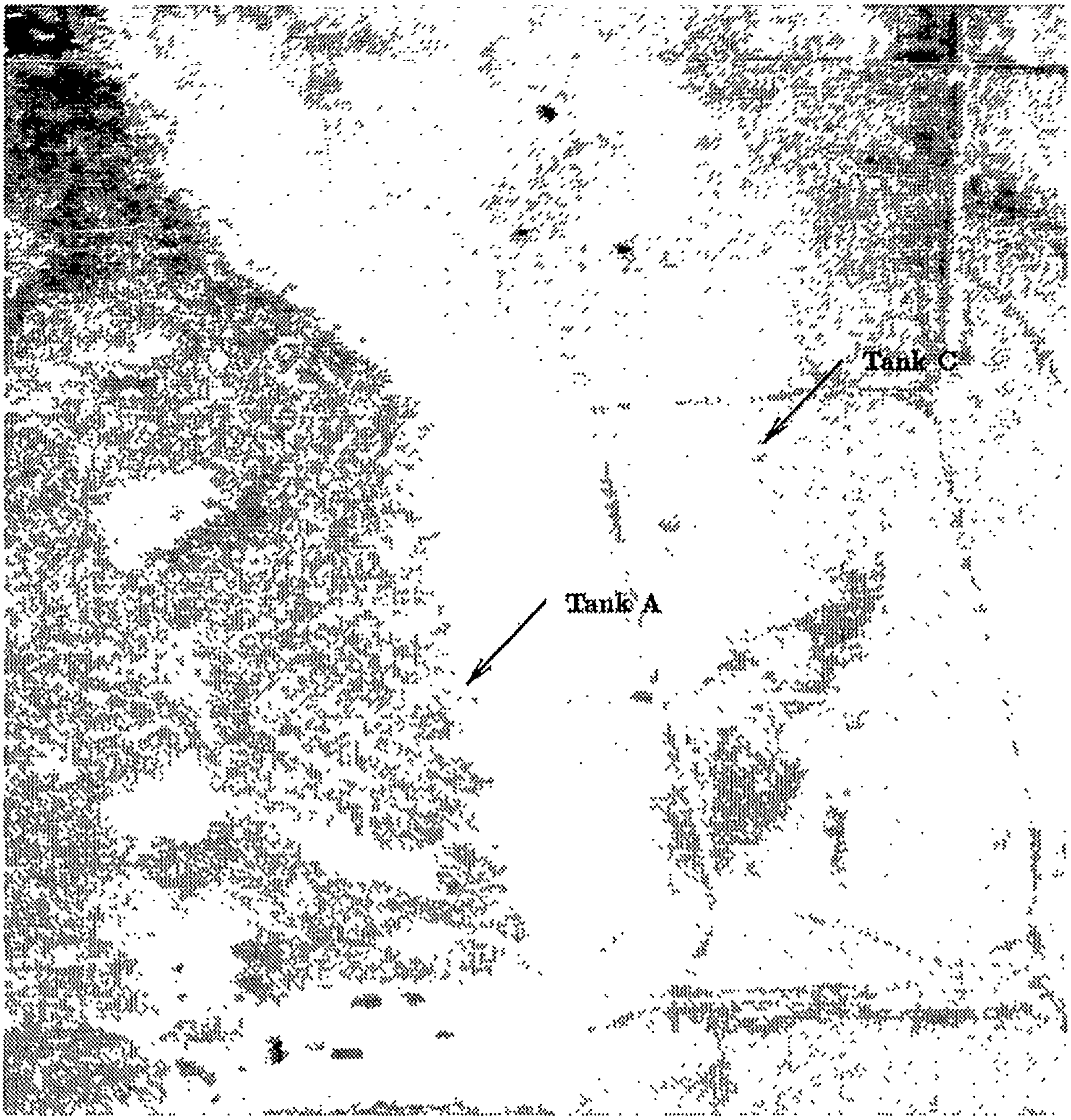

Scene consists of slightly rolling hills, with a grass-covered stretch of land surrounded by loblolly pines and deciduous trees.

Figure 9. Huntsville, Alabama—Redstone scene.

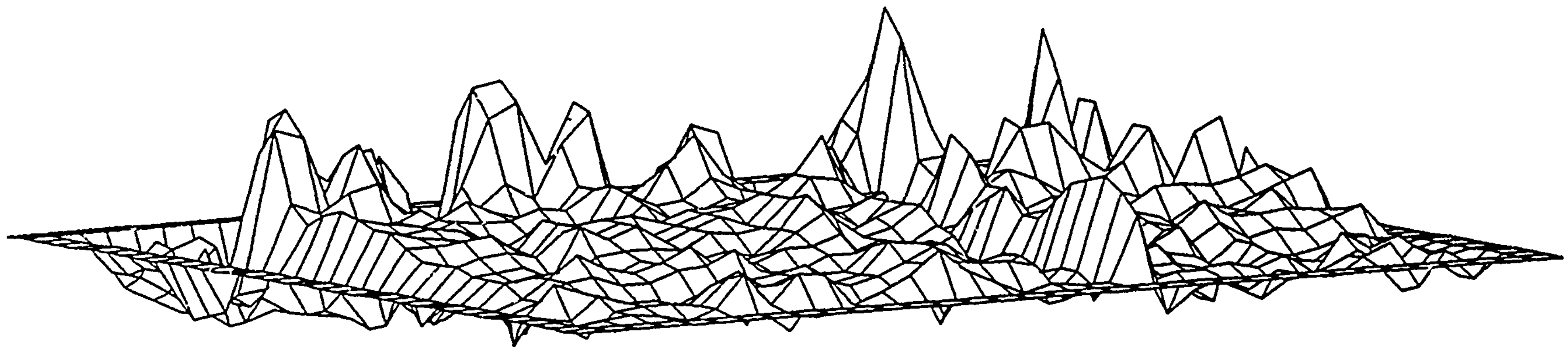

(a) Channel 4 input image; SNR = -0.93 dB.

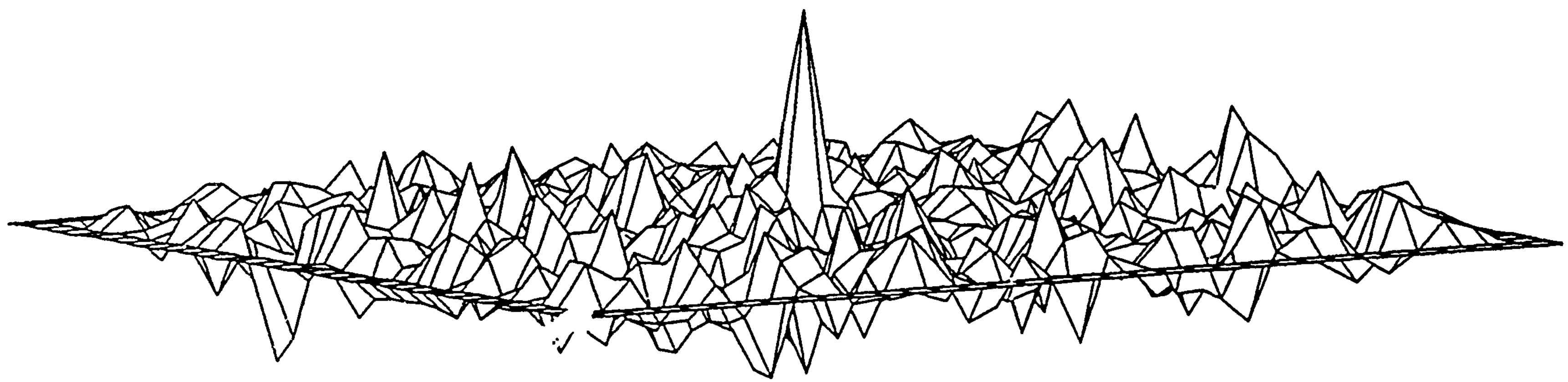

(b) Minimum noise channels 1 and 4 output image; SNR = 15.31 dB. (Preprocessed data: normalized line by line, high pass filtered, and globally normalized.)

Figure 10. Huntsville, Alabama—Redstone 2.5-m tree-line tanks.

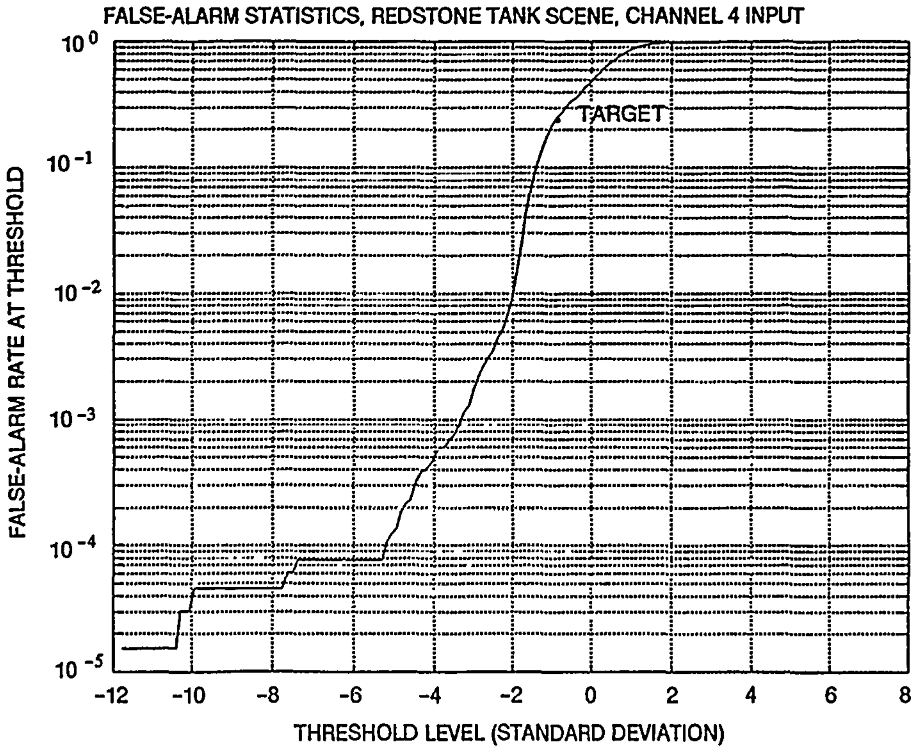

(a)

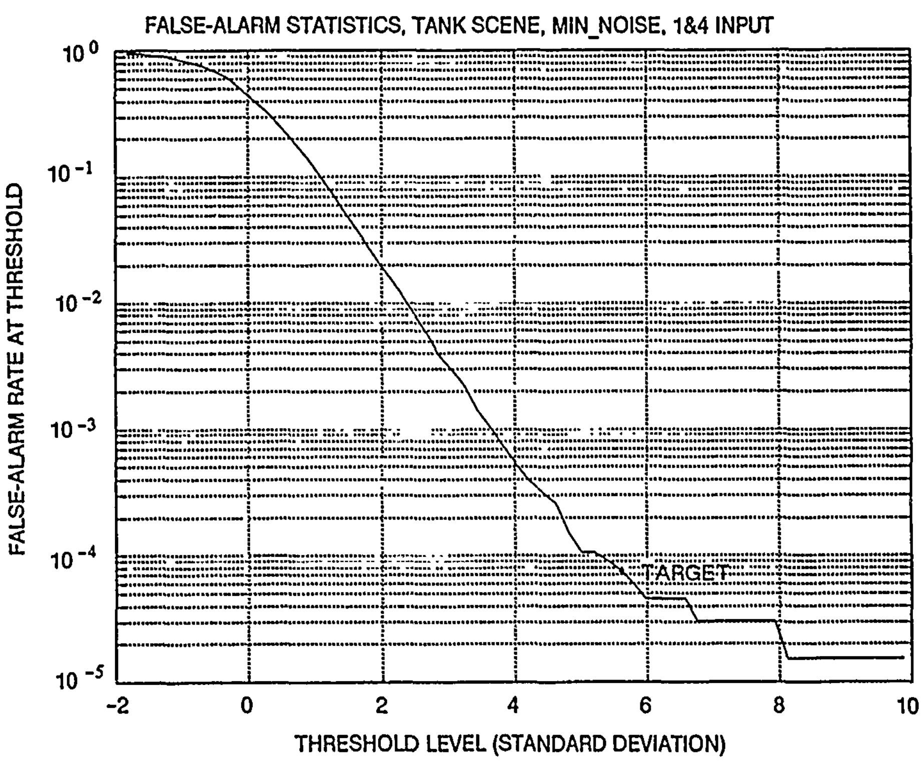

(b)

Figure 11a-b. Cumulative distributions for the unprocessed input data and preprocessed MIN_NOISE 1 and 4 output data.

These results are presented for the three algorithm variants in figure 12. The solid lines of figure 12 are plots of the theoretical output SNR for a band-to-band correlation coefficient of $\rho = 0{:}9$. The dB gain is very dependent on the color ratio. When the color ratio is 1, there is no color to the target. When the color ratio is negative, the target contrasts in the two bands have opposite signs; i.e., the target in one band is above its mean level and the target in the other band is below its mean level.

The symbols represent data points taken from targets in the Redstone scene. For these data points, the gain is plotted against the input color ratio. The data set shows an excellent match to the theory.

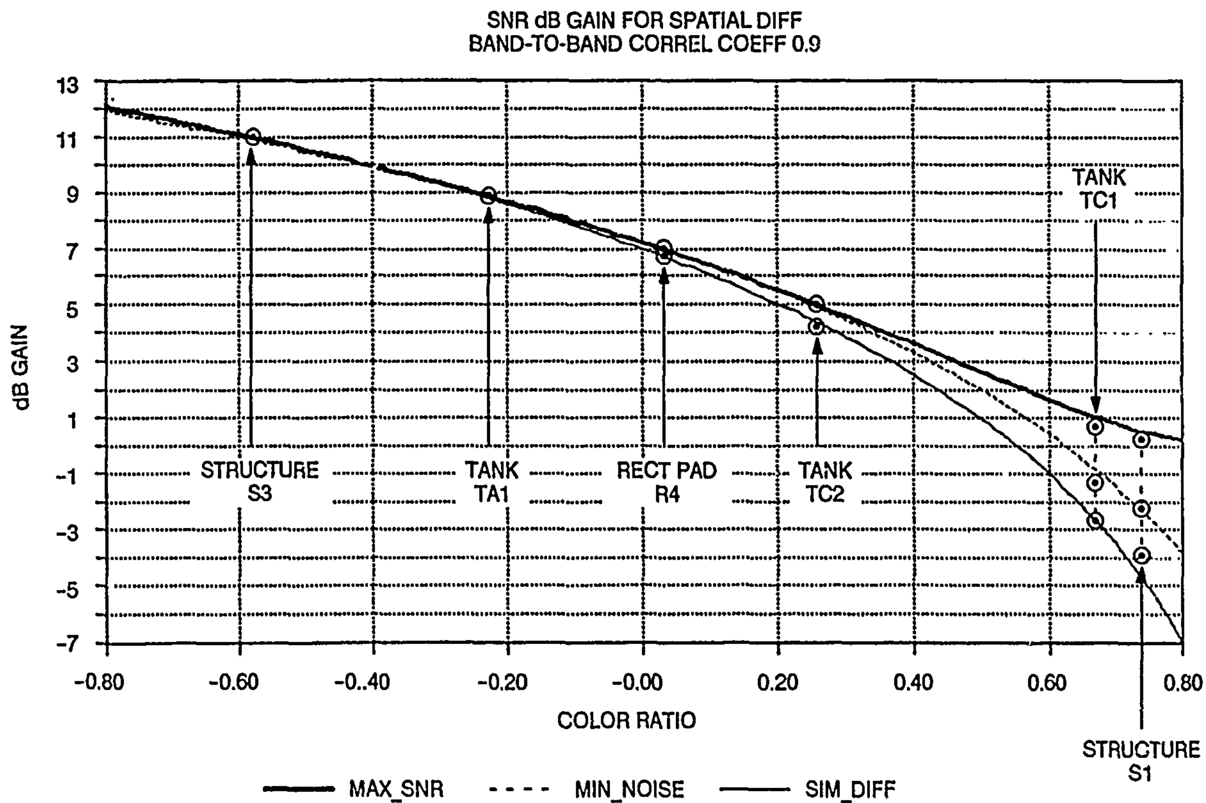

Actual data points from the Redstone scene plotted on the theoretical curves for the three variants of the weighted-difference algorithm. For this data set, preprocessing was not performed.

Figure 12. dB gain as a function of color ratio.

4.0 CONCLUSIONS

In this report, the weighted-difference algorithm was derived, analyzed, and compared to measured data. Three variants of the algorithm were evaluated: (1) simple difference; (2) minimum noise; and (3) maximum output SNR. The variants require increasing amounts of prior information to be implemented. Although the corresponding performance of the variants also increases, the increase is very small for targets that are in the detectable range of input SNR and color ratio.

The performance of the weighted-difference algorithm depends on the correlation coefficient between the two spectral bands, the ratio of the target pixels (color ratio), and the input target's

signal-to-noise ratio. In this report, the theoretical performance has been compared to measured performance for two scenes. The scenes were collected by the NASA TIMS sensor over a rural area near Adelaide, Australia and over a wooded area near the Redstone Arsenal. Scenes were selected that were 512 × 512 and 256 × 256 pixels in dimension and contained a number of targets in a cluttered background. There were 52 objects (buildings, watertanks, etc.) in the Adelaide 512 × 512 scene that were declared targets and used to evaluate the dB gain as a function of input SNR and detection statistics. There were 14 declared targets in the Adelaide 256 × 256 image that were used to evaluate SNR statistics. The analysis was repeated on the Redstone scene; however, this time there were military tanks (M60 and M48) in the scene. The Redstone scene was used to confirm the results achieved by using the Adelaide scene.

The theoretical and measured results agree extremely well. For a given correlation coefficient and color ratio, the amount of signal-to-noise ratio gain can be predicted. However, target input SNRs and color ratios can vary considerably. For the targets and scenes evaluated here, the typical gains achieved ranged from a few dB loss (targets without color) to a maximum of approximately 20 dB.

REFERENCES

1. Chan, D. S., D. A. Langan, and D. A. Staver. 1990. "Spatial Processing Techniques for the Detection of Small Targets in IR Clutter," *SPIE 1990 Conference on Optical Engineering and Photonics in Aerospace Sensing*, Conference 1305 (16–20 April), Orlando, FL.

2. Hudson, Jr., R. D., and Jacqueline W. Hudson. 1985. "The Military Applications of Remote Sensing by Infrared," *Selected Papers on Infrared Design*, SPIE vol. 513, part 1, ed. by R. Berry Johnson and William L. Wolfe, SPIE, P.O. Box 10, Bellingham, WA 98227-0010.

3. Kahle, A. B., and A. Goetz. 1983. "Mineralogic Information from a New Airborne Thermal Infrared Scanner," *Science*, vol. 222, pp. 24–27.

4. Stocker, A. D., I. S. Reed, and Xiaoli Yu. 1990. "Multi-dimensional Signal Processing for Electro-optical Target Detection," *SPIE 1990 Conference on Optical Engineering and Photonics in Aerospace Sensing, Conference 1305* (16–20 April), Orlando, FL.

5. Stotts, L. B., E. M. Winter, L. E. Hoff, and I. S. Reed. 1990. "Clutter Rejection Using Multispectral Processing," *SPIE 1990 Conference on Optical Engineering and Photonics in Aerospace Sensing, Conference 1305* (16–20 April), Orlando, FL.

6. Technical Research Associates, Inc. 1988. "Multispectral Analysis of TIMS Data," *Special Technical Report, contract DAAH01-86-C-0388, DARPA Strategic Technology Office, monitored by the U.S Army Missile Command (MICOM)* (15 December). Defense Advanced Research Projects Agency, Arlington, VA.

APPENDIX A: DETAILS OF NUMERIC RESULTS, ADELAIDE DATA SET

The TIMS Adelaide data set was processed to compare the results to the spatial difference model developed by L. E. Hoff. The first step in this processing was to determine which two of the six TIMS bands met the criterion of high correlation between the bands. A routine was run on the raw data that produces a correlation coefficient matrix as shown in figure A-1. It was also desirable for this processing that the bands be widely separated, which tends to preserve target coloring. Bands 1 and 5, with a correlation coefficient of 0.9929, were chosen.

$$\begin{pmatrix} 1.000 & 0.996 & 0.995 & 0.994 & 0.993 & 0.986 \\ 0.996 & 1.000 & 0.996 & 0.995 & 0.993 & 0.985 \\ 0.995 & 0.996 & 1.000 & 0.994 & 0.991 & 0.983 \\ 0.994 & 0.995 & 0.994 & 1.000 & 0.995 & 0.985 \\ 0.993 & 0.993 & 0.991 & 0.995 & 1.000 & 0.990 \\ 0.986 & 0.985 & 0.983 & 0.985 & 0.990 & 1.000 \end{pmatrix}$$

Figure A-1. Correlation coefficient matrix.

The second step in the processing was to window the area of interest. An area that was 256 × 256 in size was chosen. From this area, 14 target pixels were chosen for this processing run. Figure A-2 identifies the target pixels by line and column.

Pixel Name	Line	Column
a1a	133	50
a1b	133	51
a2a	137	76
a2b	137	77
a3a	162	51
a3b	163	50
a4a	57	194
a4b	58	195
a5a	237	66
a5b	237	67
a6a	245	158
a6b	246	158
a7	199	92
a8	188	235

Figure A-2. Adelaide target pixels.

Figure A-3 outlines the processing steps used on the 256 × 256 image. This diagram shows the general data flow but does not show the switches that can be made in preprocessing of the data. Three different preprocessing methods were used on this data set. The first case did a global

normalization on the image, which took the mean and variance of the entire 256 × 256 image to compute pixel values. The second case did a line-by-line normalization on the data, which entailed taking the mean and variance of each line to determine the pixel values of each, and then doing a global normalization on the data. The third case did a line-by-line normalization on the data, followed by a high-pass, 5 × 5 filter on the data. As a last step, the data set was globally normalized. The final output of the preprocessing phase of this image processing consisted of six files, three each of band 1 and band 5, globally normalized, line-by-line normalized, and filtered.

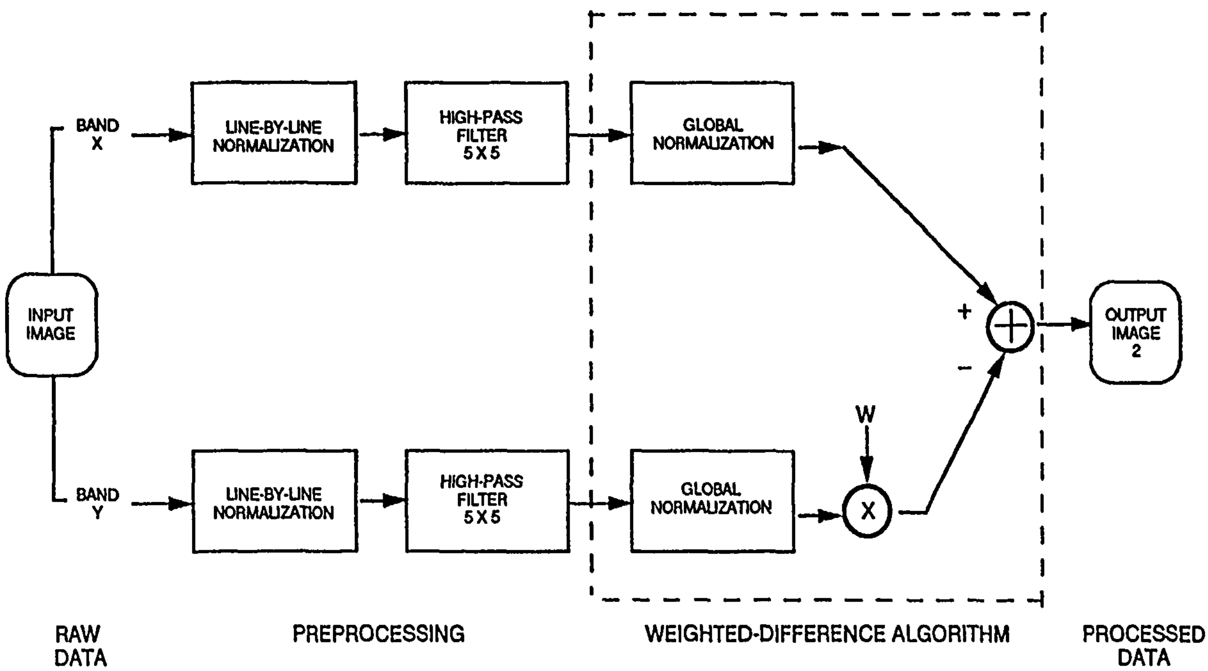

Figure A-3. Processing steps used on 256 × 256 image.

For each case, and at each target pixel, the band with the largest signal-to-noise (SNR) was determined and this data set was entered into a database (see tables A-1, A-2, and A-3). The pixel values that determined the color ratio for comparison purposes were also entered at this time.

On completion of the preprocessing steps, there were three weighted-difference algorithms applied to each set (band 1 and band 5) of data. Each of these algorithms used a different weighting factor; one maximized the output SNR, one minimized the noise, and one used a weighting factor of 1. These algorithms are referred to as Max_SNR, Min_Noise, and Sim_Diff (simple difference). The Min_Noise algorithm was applied twice to each data set. One run applied band 1 to band 5, and the second run applied band 5 to band 1. The SNR for each target pixel from each output image was then measured and entered into the database with the input band's SNRs (tables A-1 through A-3). The dB gain was then computed from the input and output SNR information and entered into the database. The data provided the necessary information for comparing the spatial-difference model to the Adelaide data.

Tables A-4, A-5, and A-6 consolidate the SNR data for each weighted difference algorithm for quick-look purposes.

Table A-1. Adelaide normalized (entire image only) target data.

NAME	LINE	PIXEL	SNR IN (dB)	BAND	PIXEL VALUE FM>SNRIN	FM<SNRIN	COLOR RATIO	SNR OUT (in dB) MAX SNR	MIN 1-5	MIN 5-1	SIMP SNR	dB GAIN MAX	MIN1-5	MIN5-1	SIMPLE
a1a	133	50	13.89994	5	-4.95455	-4.0397	0.815351	19.00481	17.39955	18.00591	17.72324	5.10	3.499	4.105	3.823
a1b	133	51	14.12785	5	-5.08627	-3.50841	0.689780	22.89334	22.27282	22.60883	22.45768	8.76	8.144	8.480	8.329
a2a	137	76	14.12785	5	-5.08627	-3.64123	0.715893	22.22293	21.49039	21.86294	21.69389	8.09	7.362	7.735	7.566
a2b	137	77	17.7531	5	-7.7208	-6.16487	0.798475	23.41788	22.04127	22.59168	22.33606	5.66	4.288	4.838	4.582
a3a	162	51	2.05	5	-1.26621	-0.71912	0.567931	13.45629	13.12955	13.35351	13.25748	11.4	11.07	11.30	11.20
a3b	163	50	4.4093	5	-1.66139	-1.11759	0.672683	13.59113	13.03079	13.34605	13.20508	9.18	8.621	8.936	8.795
a4a	57	194	15.76334	5	-6.14008	-4.96946	0.809347	21.0701	19.55179	20.1371	19.8646	5.30	3.788	4.373	4.101
a4b	58	195	16.47845	5	-6.66699	-5.10229	0.765306	23.18069	22.13463	22.59854	22.38491	6.70	5.656	6.120	5.906
a5a	237	66	14.12785	5	-5.08627	-3.64123	0.715893	22.22293	21.49039	21.86294	21.69389	8.09	7.362	7.735	7.566
a5b	237	67	10.895	5	-3.50556	-2.57865	0.735588	18.45592	17.61704	18.0219	17.83706	7.56	6.722	7.126	6.942
a6a	245	158	4.92731	5	1.76349	0.47629	0.270083	20.73613	20.62004	20.72761	20.68923	15.8	15.69	15.80	15.76
a6b	246	158	10.13666	5	3.21248	1.80452	0.561721	21.66016	21.3422	21.56212	21.46809	11.5	11.20	11.42	11.33
a7	199	92	14.41609	1	5.25792	4.92492	0.936666	15.29576	9.82421	7.93304	8.94525	0.87	-4.59	-6.48	-5.47
a8	188	235	10.82128	5	3.47593	2.20299	0.633784	20.88979	20.43851	20.71377	20.59246	10.0	9.617	9.892	9.771

Table A-2. Adelaide normalized (line by line, then entire image) target data.

NAME	LINE	PIXEL	> SNR IN (dB)	BAND	PIXEL VALUE FM>SNRIN	FM<SNRIN	COLOR RATIO	SNR OUT (In dB) MAX SNR	MIN 1-5	MIN 5-1	SIMP SNR	dB GAIN MAX	MIN1-5	MIN5-1	SIMPLE
a1a	133	50	16.9625	5	-7.04896	-5.74561	0.815100	20.51602	17.98848	19.00943	18.5398	3.55	1.025	2.046	1.577
a1b	133	51	17.41588	5	-7.42667	-5.04628	0.679480	24.43176	23.46915	24.01368	23.77154	7.01	6.053	6.597	6.355
a2a	137	76	16.3477	5	-6.56728	-5.12228	0.779969	20.87023	18.97939	19.82043	19.43594	4.52	2.631	3.472	3.088
a2b	137	77	20.49391	5	-10.5851	-9.23216	0.872183	22.44913	18.04218	19.56755	18.86422	1.95	-2.45	-0.92	-1.62
a3a	162	51	9.2242	5	-2.89208	-2.00616	0.693673	15.91557	14.86855	15.44315	15.18646	6.69	5.644	6.218	5.962
a3b	163	50	11.31666	5	-3.67987	-2.88053	0.782780	15.76314	13.83025	14.68353	14.29322	4.44	2.513	3.366	2.976
a4a	57	194	18.78598	5	-8.69359	-7.22343	0.830700	21.90009	18.99117	20.11604	19.59766	3.11	0.205	1.330	0.811
a4b	58	195	19.77904	5	-9.74882	-7.59554	0.779124	24.32445	22.44597	23.28338	22.90062	4.54	2.666	3.504	3.121
a5a	237	66	17.88702	5	-7.84063	-5.73463	0.731399	23.67152	22.34047	23.01044	22.70777	5.78	4.453	5.123	4.820
a5b	237	67	14.70665	5	-5.43666	-4.10791	0.755594	19.87536	18.30028	19.04694	18.70749	5.16	3.593	4.340	4.000
a6a	245	158	-0.97518	5	0.8938	-0.42181	-0.47192	18.62448	18.57658	18.61391	18.62112	19.5	19.55	19.58	19.59
a6b	246	158	9.01323	5	2.82268	1.22893	0.435377	20.45167	20.12804	20.39219	20.28698	11.4	11.11	11.37	11.27
a7	199	92	13.04324	1	4.48913	3.85296	0.858286	15.38112	12.93983	11.57497	12.31004	2.33	-0.10	-1.46	-0.73
a8	188	235	9.62549	5	3.02883	1.27447	0.420779	21.27448	20.96671	21.22159	21.12094	11.6	11.34	11.59	11.49

Table A-3. Adelaide (normalized line by line/high-pass filter/then renormalized) target data.

NAME	LINE	PIXEL	> SNR IN (dB)	BAND	PIXEL VALUE FM>SNRIN	FM<SNRIN	COLOR RATIO	SNR OUT (in dB) MAX SNR	MIN 1-5	MIN 5-1	SIMP SNR	dB GAIN MAX	MIN1-5	MIN5-1	SIMPLE
a1a	133	50	12.67837	5	-4.30446	-3.60454	0.837396	17.48344	15.73921	16.33727	16.05657	4.80	3.060	3.658	3.378
a1b	133	51	12.91727	5	-4.4245	-3.10256	0.701222	21.98891	21.41471	21.71597	21.57983	9.07	8.497	8.798	8.662
a2a	137	76	12.05138	5	-4.00469	-3.0098	0.751568	19.72355	18.90941	19.28246	19.11112	7.67	6.858	7.231	7.059
a2b	137	77	15.79074	5	-6.15938	-5.20829	0.845586	20.28915	18.38488	19.0175	18.72013	4.49	2.594	3.226	2.929
a3a	162	51	0.54261	5	-1.06446	-0.50388	0.473366	14.23086	14.04098	14.18896	14.12847	13.6	13.49	13.64	13.58
a3b	163	50	3.05813	5	-1.42202	-0.92494	0.650440	13.36969	12.94531	13.19509	13.08428	10.3	9.887	10.13	10.02
a4a	57	194	15.8731	5	-6.21806	-5.17281	0.831900	20.88108	19.23371	19.81047	19.54006	5.00	3.360	3.937	3.666
a4b	58	195	16.69225	5	-6.83302	-5.4085	0.791524	23.11026	21.9855	22.44024	22.22903	6.41	5.293	5.747	5.536
a5a	237	66	13.26106	5	-4.60313	-3.33905	0.725386	21.68434	21.01014	21.34256	21.19112	8.42	7.749	8.081	7.930
a5b	237	67	10.09843	5	-3.19832	-2.38544	0.745841	17.93947	17.15941	17.52285	17.35621	7.84	7.060	7.424	7.257
a6a	245	158	1.71528	5	1.21833	0.16471	0.135193	19.63205	19.56133	19.63073	19.60928	17.9	17.84	17.91	17.89
a6b	246	150	7.92423	5	2.49007	1.29809	0.521306	20.81269	20.58337	20.75147	20.68101	12.8	12.65	12.82	12.75
a7	199	92	13.37001	1	4.66122	4.3944	0.942757	14.22003	8.52137	6.71919	6.68011	0.85	-4.84	-6.65	-6.68
a8	188	235	9.73667	5	3.06785	1.91201	0.623241	20.65253	20.28568	20.5136	20.41357	10.9	10.54	10.77	10.67

Table A-4. SNRs for various processing (normalized only, normalized line by line, filtered) maximum SNR—Adelaide channels 1 and 5 (8/15/90).

NAME	LINE	PIXEL	> SNR IN (dB) BAND	VALUE	NORMALIZED WHOLE IMAGE	NORMALIZED LN X LN	HIGH PASS FILTER
a1a	133	50	5	13.89994	19.00481	17.48344	20.51602
a1b	133	51	5	14.12785	22.89334	21.98891	24.43176
a2a	137	76	5	14.12785	22.22293	19.72355	20.87023
a2b	137	77	5	17.7531	23.41788	20.28915	22.44913
a3a	162	51	5	2.05	13.45629	14.23086	15.91557
a3b	163	50	5	4.4093	13.59113	13.36969	15.76314
a4a	57	194	5	15.76334	21.0701	20.88108	21.90009
a4b	58	195	5	16.47845	23.18069	23.11026	24.32445
a5a	237	66	5	14.12785	22.22293	21.68434	23.67152
a5b	237	67	5	10.895	18.45592	17.93947	19.87536
a6a	245	158	5	4.92731	20.73613	19.63205	18.62448
a6b	246	158	5	10.13666	21.66016	20.81269	20.45167
a7	199	92	1	14.41609	15.29576	14.22003	15.38112
a8	188	235	5	10.82128	20.88979	20.65253	21.27448

Table A-5. SNRs for various processing (normalized only, normalized line by line, filtered) minimum noise—Adelaide channels 1 and 5 (8/15/90).

NAME	LINE	PIXEL	> SNR IN (dB) BAND	VALUE	NORMALIZED WHOLE IMAGE	NORMALIZED LN X LN	HIGH PASS FILTER
a1a	133	50	5	13.89994	17.39955	15.73921	17.98848
a1b	133	51	5	14.12785	22.27282	21.41471	23.46915
a2a	137	76	5	14.12785	21.49039	18.90941	18.97939
a2b	137	77	5	17.7531	22.04127	18.38488	18.04218
a3a	162	51	5	2.05	13.12955	14.04098	14.86855
a3b	163	50	5	4.4093	13.03079	12.94531	13.83025
a4a	57	194	5	15.76334	19.55179	19.23371	18.99117
a4b	58	195	5	16.47845	22.13463	21.9855	22.44597
a5a	237	66	5	14.12785	21.49039	21.01014	22.34047
a5b	237	67	5	10.895	17.61704	17.15941	18.30028
a6a	245	158	5	4.92731	20.62004	19.56133	18.57658
a6b	246	158	5	10.13666	21.3422	20.58337	20.12804
a7	199	92	1	14.41609	9.82421	8.52137	12.93983
a8	188	235	5	10.82128	20.43851	20.28568	20.96671

Table A-6. SNRs for various processing (normalized only, normalized line by line, filtered) simple difference—Adelaide channels 1 and 5 (8/15/90).

NAME	LINE	PIXEL	> SNR IN (dB) BAND	VALUE	NORMALIZED WHOLE IMAGE	NORMALIZED LN X LN	HIGH PASS FILTER
a1a	133	50	5	13.89994	17.72324	16.05657	18.5398
a1b	133	51	5	14.12785	22.45768	21.57983	23.77154
a2a	137	76	5	14.12785	21.69389	19.11112	19.43594
a2b	137	77	5	17.7531	22.33606	18.72013	18.86422
a3a	162	51	5	2.05	13.25748	14.12847	15.18646
a3b	163	50	5	4.4093	13.20508	13.08428	14.29322
a4a	57	194	5	15.76334	19.8646	19.54006	19.59766
a4b	58	195	5	16.47845	22.38491	22.22903	22.90062
a5a	237	66	5	14.12785	21.69389	21.19112	22.70777
a5b	237	67	5	10.895	17.83706	17.35621	18.70749
a6a	245	158	5	4.92731	20.68923	19.60928	18.62112
a6b	246	158	5	10.13666	21.46809	20.68101	20.28698
a7	199	92	1	14.41609	8.94525	6.68011	12.31004
a8	188	235	5	10.82128	20.59246	20.41357	21.12094

APPENDIX B: MODEL FOR TWO-CHANNEL SYSTEM

The following is a model for a two-channel system. Let

$$R_k = S_k \text{ or } N_k \qquad k = 1, 2$$

be the received radiance in band k. If signal is present, the background, N_k, is occluded. The spatial difference algorithm is formulated as

$$d(R) = R_1 - \omega R_2 .$$

For the signal pixel(s), we get

$$d(S) = S_1 - \omega S_2$$

and for the background pixels (noise and clutter), we get

$$d(N) = N_1 + \omega N_2 .$$

The output SNR is defined as follows

$$\text{SNR} = \frac{|d(S)|^2}{var[d(N)]} .$$

Assume that each channel input has been normalized so that image mean is zero and the variance is 1.0. Define the following two parameters:

$$c = \frac{S_2}{S_1}, \qquad \text{where } S_2 < S_1 , \qquad -1 < c < 1$$

$$\rho = \frac{Cov[N_1, N_2]}{\sigma_1 \sigma_2} .$$

First, let us derive the SNR:

$$\begin{aligned} var[d(N)] &= E[(N_1 - \omega N_2)^2] \\ &= E[N_1^2 - 2\omega N_1 N_2 + \omega^2 N_2^2] \\ &= \sigma_1^2 - 2\omega\rho\sigma_1\sigma_2 + \omega^2\sigma_2^2 \\ &= 1 - 2\omega\rho + \omega^2 \end{aligned}$$

and

$$S_{ni} = \frac{(S_i - m_i)}{\sigma_i} \qquad i = 1, 2$$

giving

$$\text{SNR} = \frac{(S_{n1} - \omega S_{n2})^2}{(1 - 2\omega\rho + \omega^2)} = \frac{S_{n1}^2 (1 - \omega c)^2}{1 - 2\omega\rho + \omega^2} .$$

We derive ω three ways: (1) choose ω to maximize SNR; (2) choose ω to minimize $Var[d(N)]$; (3) choose ω equal to 1. To find the ω that maximizes the SNR, we perform the following derivations:

$$\frac{\partial \mathrm{SNR}}{\partial \omega} = \frac{2S_{n1}^2(1 - \omega c)(-c)}{1 - 2\omega\rho + \omega^2} + \frac{S_{n1}^2(1 - \omega c)^2}{(1 - 2\omega\rho + \omega^2)^2}(2\omega - 2\rho)(-1)$$

$$= \frac{-S_{n1}^2(1 - \omega c)}{1 - 2\omega\rho + \omega^2}\left[2c + \frac{(1 - \omega c)(2\omega - 2\rho)}{1 - 2\omega\rho + \omega^2}\right]$$

$$= \frac{-2S_{n1}^2(1 - \omega c)}{1 - 2\omega\rho + \omega^2}\left[c + \frac{(1 - \omega c)(\omega - \rho)}{1 - 2\omega\rho + \omega^2}\right].$$

The above equation has two zeros. The first one, easily seen in the first term, is $\omega = 1/c$. The second one is derived as follows:

$$\frac{(1 - \omega c)(\omega - \rho)}{1 - 2\omega\rho + \omega^2} + c = \frac{\omega - \omega^2 c - \rho + \omega c\rho + c - 2\omega c\rho + \omega^2 c}{1 - 2\omega\rho + \omega^2}$$

$$= \frac{\omega + c - \omega c\rho - \rho}{1 - 2\omega\rho + \omega^2}$$

$$= \frac{\omega(1 - c\rho) + c - \rho}{1 - 2\omega\rho + \omega^2}$$

which, when we set equal to zero, gives

$$\omega = \frac{\rho - c}{1 - \rho c}.$$

The first term gives a minimum, the second a maximum. Figure B-1 is a plot of SNR as a function of ω, showing the maximum and minimum. This plot has ρ equal to 0.99 and c equal to 0.9. For case 2 we take the derivative of the noise term with respect to ω.

$$\frac{\partial Var[d(N)]}{\partial \omega} = -2\rho - 2\omega \Rightarrow \rho = \omega$$

and

$$\mathrm{SNR} = S_{nx}^2 \frac{(1 - \rho c)^2}{1 - \rho^2}.$$

For case 3, we just set $\omega = 1$, giving

$$\mathrm{SNR} = \frac{S_{nx}^2(1 - c)^2}{2(1 - \rho)}.$$

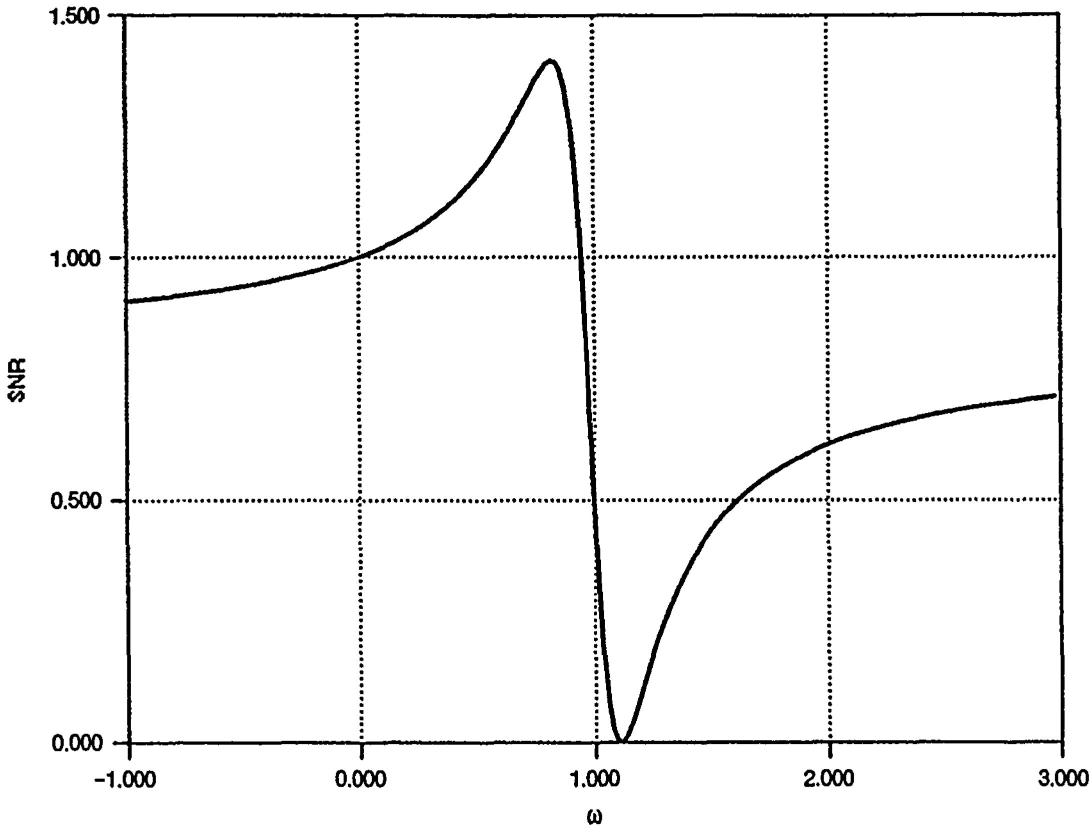

Figure B-1. SNR as a function of ω; $\rho = 0.99$, $c = 0.90$.

APPENDIX C: ANALYSIS OF DATA, ADELAIDE 512 $\times$ 512 SCENE

The TIMS Adelaide 512 $\times$ 512 data set was analyzed to evaluate detection statistics for 10^{-3} and 10^{-4} false-alarm rates as a follow-on to investigation of weighted-difference signal-processing algorithms for detecting g und targets by using dual-band IR data. Extensive investigation of these algorithms was done by using the TIMS Adelaide 256 $\times$ 256 data set; however, for determining detection statistics, the TIMS Adelaide 512 $\times$ 512 image was chosen because it contained significantly more targets. Figure C-1 identifies these targets by row and column number.

Line	Pixel	Pixel Name	Line	Pixel	Pixel Name
133	50	A1A	463	160	A21
133	51	A1B	454	182	A22
137	76	A2A	441	203	A23
137	77	A2B	432	204	A24
162	51	A3A	428	211	A25
163	50	A3B	393	155	A26
57	194	A4A	377	216	A27
58	195	A4B	346	250	A28
237	66	A5A	285	207	A29
237	67	A5B	262	192	A30
245	158	A6A	418	280	A31
246	158	A6B	420	311	A32
199	92	A7	440	302	A33
188	235	A8	478	256	A34
259	119	A9	454	392	A35
298	90	A10	492	395	A36
322	97	A11	489	401	A37
360	107	A12	478	498	A38
403	7	A13	9	330	A39
382	32	A14	98	291	A40
417	32	A15	118	303	A41
404	40	A16	170	341	A42
474	8	A17	121	373	A43
506	149	A18	183	434	A44
508	171	A19	198	435	A45
475	140	A20	272	413	A46

Figure C-1. TIMS Adelaide 512 $\times$ 512 image targets.

The detection statistics were determined for two sets of data: data that had not been preprocessed and preprocessed data. The preprocessed data set was line-by-line normalized, filtered with a high-pass filter, and then globally normalized. There were two weighted-difference algorithms, simple difference and minimum noise, applied to each set.

Histograms were formed for each image after omitting the 52 targets. Two accumulated statistics were obtained for each histogram: ascending values and descending values. These accumulated statistics were used to estimate the false-alarm rate associated with each target. The threshold for the false-alarm rates was then obtained from the data. Attachment (1), which follows table C-10, contains the numeric results of this computation. At the predetermined thresholds of 10^{-3} and 10^{-4} , the number of detections that occurred was determined by using previously measured pixel values in tables C-1 through C-10. This determination included targets that were positive, with a pixel value larger than the

image mean, and negative targets, with a pixel value less than the mean. Figure C-2 summarizes the results.

Processing Algorithm (Bands 1 and 5)	Detections at CFAR 10^{-3}	10^{-4}
No Preprocessing		
Band 5—Raw Input	28	20
Simple Difference	44	18
Minimum Noise	45	18
Preprocessed		
Band 5	34	19
Simple Difference	47	23
Minimum Noise	47	19

Figure C-2. Detection statistics for 52 targets in the Adelaide scene.

Table C-1. Channel 1, no preprocessing.

Line	Pixel	Name	Pixel val	Local SNR	Global SNR
133	50	A1A	59.00000	11.64553	10.83174
133	51	A1B	63.00000	10.68036	9.76055
137	76	A2A	62.00000	12.22594	10.04098
137	77	A2B	43.00000	16.63482	14.14314
162	51	A3A	84.00000	-1.43988	-0.38641
163	50	A3B	81.00000	1.53535	2.00270
57	194	A4A	52.00000	12.56733	12.43736
58	195	A4B	51.00000	12.63880	12.64430
237	66	A5A	62.00000	10.32106	10.04098
237	67	A5B	70.00000	7.74971	7.49383
245	158	A6A	93.00000	-23.70481	-26.37514
246	158	A6B	103.00000	3.53570	-0.34164
199	92	A7	129.00000	10.89036	11.09208
188	235	A8	106.00000	2.80526	2.03672
259	119	A9	64.00000	11.30198	9.47076
298	90	A10	40.00000	16.17731	14.64463
322	97	A11	43.00000	16.39803	14.14314
360	107	A12	63.00000	10.03833	9.76055
403	7	A13	133.00000	17.36060	12.01885
382	32	A14	69.00000	10.67624	7.85616
417	32	A15	62.00000	13.89731	10.04098
404	40	A16	59.00000	13.12808	10.83174
474	8	A17	134.00000	15.68090	12.23588
506	149	A18	47.00000	15.95534	13.42601
508	171	A19	39.00000	16.21332	14.80555
475	140	A20	72.00000	9.27506	6.72040
463	160	A21	154.00000	16.62390	15.72015
454	182	A22	167.00000	15.79108	17.41017
441	203	A23	76.00000	7.53977	4.93013
432	204	A24	164.00000	17.55718	17.04832
428	211	A25	87.00000	-1.42042	-3.69298
393	155	A26	75.00000	6.84302	5.41346
377	216	A27	167.00000	16.23982	17.41017
346	250	A28	122.00000	10.70919	9.18588
285	207	A29	63.00000	12.31237	9.76055
262	192	A30	63.00000	10.28495	9.76055
418	280	A31	117.00000	5.72776	7.51193
420	311	A32	70.00000	9.19157	7.49383
440	302	A33	50.00000	14.35641	12.84642
478	256	A34	117.00000	7.50255	7.51193
454	392	A35	126.00000	8.33095	10.32574
492	395	A36	56.00000	13.44685	11.55648
489	401	A37	127.00000	9.00575	10.58877
478	498	A38	89.00000	-9.69323	-6.90161
9	330	A39	119.00000	6.50417	8.22067
98	291	A40	44.00000	12.83869	13.96933
118	303	A41	64.00000	9.10144	9.47076
170	341	A42	115.00000	10.04106	6.74018
121	373	A43	67.00000	9.16296	8.53842
183	434	A44	112.00000	-3.26578	5.43645
198	435	A45	124.00000	8.41299	9.77449
272	413	A46	56.00000	12.40393	11.55648

Table C-2. Channel 5, no preprocessing.

Line	Pixel	Name	Pixel val	Local SNR	Global SNR
133	50	A1A	96.00000	14.89897	14.52934
133	51	A1B	94.00000	15.27888	14.90951
137	76	A2A	97.00000	15.74141	14.33283
137	77	A2B	70.00000	19.94801	18.51143
162	51	A3A	118.00000	9.78546	8.64409
163	50	A3B	113.00000	11.36008	10.37303
57	194	A4A	94.00000	14.41450	14.90951
58	195	A4B	85.00000	15.79175	16.44022
237	66	A5A	80.00000	18.42231	17.18686
237	67	A5B	99.00000	15.11119	13.92594
245	158	A6A	148.00000	0.48357	-1.21316
246	158	A6B	162.00000	9.86171	8.08956
199	92	A7	172.00000	10.05867	11.43312
188	235	A8	164.00000	7.80173	8.86916
259	119	A9	97.00000	15.38368	14.33283
298	90	A10	53.00000	19.34751	20.38299
322	97	A11	33.00000	20.47749	22.16727
360	107	A12	75.00000	19.52915	17.87437
403	7	A13	188.00000	16.25512	15.01965
382	32	A14	101.00000	13.90491	13.49905
417	32	A15	82.00000	16.34279	16.89586
404	40	A16	69.00000	17.22554	18.63342
474	8	A17	194.00000	16.62584	16.05701
506	149	A18	54.00000	18.84574	20.28338
508	171	A19	49.00000	20.14812	20.77038
475	140	A20	95.00000	14.24431	14.72151
463	160	A21	213.00000	16.37731	18.70532
454	182	A22	190.00000	12.12395	15.37938
441	203	A23	102.00000	11.26938	13.27747
432	204	A24	197.00000	14.43143	16.53265
428	211	A25	122.00000	4.90524	6.96057
393	155	A26	138.00000	-13.12124	-9.84341
377	216	A27	223.00000	17.18371	19.83058
346	250	A28	160.00000	5.10370	7.23303
285	207	A29	96.00000	14.40050	14.52934
262	192	A30	93.00000	13.03213	15.09353
418	280	A31	133.00000	-1.03939	-0.74510
420	311	A32	79.00000	15.60697	17.32878
440	302	A33	77.00000	16.82623	17.60586
478	256	A34	138.00000	-11.40859	-9.84341
454	392	A35	152.00000	0.36730	2.58281
492	395	A36	65.00000	16.63120	19.10495
489	401	A37	160.00000	4.95219	7.23303
478	498	A38	144.00000	-10.54844	-8.11226
9	330	A39	151.00000	-1.88051	1.77783
98	291	A40	25.00000	21.08889	22.78962
118	303	A41	78.00000	15.47009	17.46843
170	341	A42	162.00000	8.64341	8.08956
121	373	A43	85.00000	13.50184	16.44022
183	434	A44	131.00000	-0.26179	1.26005
198	435	A45	150.00000	-0.80553	0.89056
272	413	A46	58.00000	16.75670	19.87312

Table C-3. Channel 1, preprocessed.

Line	Pixel	Name	Pixel val	Local SNR	Global SNR
133	50	A1A	87.00000	13.18351	12.39540
133	51	A1B	92.00000	11.99214	11.17592
137	76	A2A	90.00000	13.72329	11.68443
137	77	A2B	62.00000	18.80811	16.77104
162	51	A3A	108.00000	6.70344	5.45678
163	50	A3B	102.00000	9.15027	8.05970
57	194	A4A	84.00000	12.56092	13.05255
58	195	A4B	81.00000	12.96470	13.66346
237	66	A5A	77.00000	16.00595	14.41642
237	67	A5B	90.00000	13.20043	11.68443
245	158	A6A	122.00000	-7.34266	-9.21409
246	158	A6B	135.00000	2.35190	0.61036
199	92	A7	165.00000	11.24455	12.76449
188	235	A8	135.00000	-0.53703	0.61036
259	119	A9	91.00000	12.86638	11.43389
298	90	A10	50.00000	17.92134	18.28168
322	97	A11	31.00000	18.97251	20.23900
360	107	A12	72.00000	17.65183	15.27419
403	7	A13	185.00000	17.86539	16.29877
382	32	A14	94.00000	11.54459	10.63577
417	32	A15	70.00000	15.79424	15.59491
404	40	A16	63.00000	15.86881	16.63244
474	8	A17	192.00000	18.07628	17.25985
506	149	A18	56.00000	16.68670	17.55916
508	171	A19	51.00000	18.36644	18.16535
475	140	A20	89.00000	11.64286	11.92794
463	160	A21	217.00000	17.64830	20.02016
454	182	A22	185.00000	12.96514	16.29877
441	203	A23	95.00000	8.28025	10.35255
432	204	A24	201.00000	16.21811	18.35726
428	211	A25	112.00000	1.09238	3.15332
393	155	A26	122.00000	-11.46995	-9.21409
377	216	A27	223.00000	17.88440	20.56992
346	250	A28	154.00000	7.85478	9.95705
285	207	A29	91.00000	11.99037	11.43389
262	192	A30	83.00000	11.25739	13.26099
418	280	A31	130.00000	-6.61097	-5.56314
420	311	A32	78.00000	12.99186	14.23421
440	302	A33	73.00000	14.81421	15.10928
478	256	A34	144.00000	5.54500	6.25693
454	392	A35	151.00000	6.36485	9.00260
492	395	A36	55.00000	15.00566	17.68383
489	401	A37	158.00000	8.60537	11.08563
478	498	A38	129.00000	-9.33133	-7.57882
9	330	A39	135.00000	-3.37199	0.61036
98	291	A40	23.00000	19.80061	20.94721
118	303	A41	75.00000	13.40707	14.76975
170	341	A42	145.00000	7.00428	6.70641
121	373	A43	76.00000	12.10294	14.59488
183	434	A44	126.00000	-22.26839	-20.87355
198	435	A45	144.00000	4.53005	6.25693
272	413	A46	53.00000	15.09171	17.92793

Table C-4. Channel 5, preprocessed.

Line	Pixel	Name	Pixel val	Local SNR	Global SNR
133	50	A1A	96.00000	14.89897	14.52934
133	51	A1B	94.00000	15.27888	14.90951
137	76	A2A	97.00000	15.74141	14.33283
137	77	A2B	70.00000	19.94801	18.51143
162	51	A3A	118.00000	9.78546	8.64409
163	50	A3B	113.00000	11.36008	10.37303
57	194	A4A	94.00000	14.41450	14.90951
58	195	A4B	85.00000	15.79175	16.44022
237	66	A5A	80.00000	18.42231	17.18686
237	67	A5B	99.00000	15.11119	13.92594
245	158	A6A	148.00000	0.48357	-1.21316
246	158	A6B	162.00000	9.86171	8.08956
199	92	A7	172.00000	10.05867	11.43312
188	235	A8	164.00000	7.80173	8.86916
259	119	A9	97.00000	15.38368	14.33283
298	90	A10	53.00000	19.34751	20.38299
322	97	A11	33.00000	20.47749	22.16727
360	107	A12	75.00000	19.52915	17.87437
403	7	A13	188.00000	16.25512	15.01965
382	32	A14	101.00000	13.90491	13.49905
417	32	A15	82.00000	16.34279	16.89586
404	40	A16	69.00000	17.22554	18.63342
474	8	A17	194.00000	16.62584	16.05701
506	149	A18	54.00000	18.84574	20.28338
508	171	A19	49.00000	20.14812	20.77038
475	140	A20	95.00000	14.24431	14.72151
463	160	A21	213.00000	16.37731	18.70532
454	182	A22	190.00000	12.12395	15.37938
441	203	A23	102.00000	11.26938	13.27747
432	204	A24	197.00000	14.43143	16.53265
428	211	A25	122.00000	4.90524	6.96057
393	155	A26	138.00000	-13.12124	-9.84341
377	216	A27	223.00000	17.18371	19.83058
346	250	A28	160.00000	5.10370	7.23303
285	207	A29	96.00000	14.40050	14.52934
262	192	A30	93.00000	13.03213	15.09353
418	280	A31	133.00000	-1.03939	-0.74510
420	311	A32	79.00000	15.60697	17.32878
440	302	A33	77.00000	16.82623	17.60586
478	256	A34	138.00000	-11.40859	-9.84341
454	392	A35	152.00000	0.36730	2.58281
492	395	A36	65.00000	16.63120	19.10495
489	401	A37	160.00000	4.95219	7.23303
478	498	A38	144.00000	-10.54844	-8.11226
9	330	A39	151.00000	-1.88051	1.77783
98	291	A40	25.00000	21.08889	22.78962
118	303	A41	78.00000	15.47009	17.46843
170	341	A42	162.00000	8.64341	8.08956
121	373	A43	85.00000	13.50184	16.44022
183	434	A44	131.00000	-0.26179	1.26005
198	435	A45	150.00000	-0.80553	0.89056
272	413	A46	58.00000	16.75670	19.87312

Table C-5. Minimum noise, channels 1 and 5, no preprocessing.

Line	Pixel	Name	Pixel val	Local SNR	Global SNR
133	50	A1A	31.00000	15.38540	15.36220
133	51	A1B	36.00000	19.46432	19.96654
137	76	A2A	35.00000	19.01599	19.22065
137	77	A2B	36.00000	19.92917	19.96654
162	51	A3A	28.00000	14.42188	10.63891
163	50	A3B	28.00000	14.43850	10.63891
57	194	A4A	33.00000	17.83999	17.50394
58	195	A4B	36.00000	20.49207	19.96654
237	66	A5A	35.00000	20.54815	19.22065
237	67	A5B	31.00000	16.87674	15.36220
245	158	A6A	14.00000	19.90649	18.14034
246	158	A6B	13.00000	20.90228	18.98038
199	92	A7	27.00000	11.34620	8.24558
188	235	A8	15.00000	17.34940	17.21027
259	119	A9	32.00000	18.48232	16.49891
298	90	A10	38.00000	20.81809	21.28993
322	97	A11	38.00000	21.70469	21.28993
360	107	A12	33.00000	18.79750	17.50394
403	7	A13	28.00000	15.85151	10.63891
382	32	A14	30.00000	17.24889	14.05400
417	32	A15	28.00000	13.00053	10.63891
404	40	A16	33.00000	17.90347	17.50394
474	8	A17	29.00000	14.26094	12.51323
506	149	A18	36.00000	12.17385	19.96654
508	171	A19	35.00000	12.32998	19.22065
475	140	A20	31.00000	17.85920	15.36220
463	160	A21	33.00000	19.47829	17.50394
454	182	A22	30.00000	15.31729	14.05400
441	203	A23	32.00000	16.30754	16.49891
432	204	A24	36.00000	19.45976	19.96654
428	211	A25	26.00000	5.50052	4.93086
393	155	A26	32.00000	10.96959	16.49891
377	216	A27	29.00000	13.74139	12.51323
346	250	A28	31.00000	17.98290	15.36220
285	207	A29	35.00000	19.60094	19.22065
262	192	A30	30.00000	13.99266	14.05400
418	280	A31	28.00000	7.30920	10.63891
420	311	A32	36.00000	18.22665	19.96654
440	302	A33	37.00000	18.25457	20.65342
478	256	A34	36.00000	18.75273	19.96654
454	392	A35	36.00000	20.42850	19.96654
492	395	A36	33.00000	17.09636	17.50394
489	401	A37	33.00000	17.33883	17.50394
478	498	A38	24.00000	-5.41655	-18.08220
9	330	A39	26.00000	1.53669	4.93086
98	291	A40	41.00000	22.11342	22.95985
118	303	A41	37.00000	18.09341	20.65342
170	341	A42	20.00000	7.67877	9.97790
121	373	A43	32.00000	6.49315	16.49891
183	434	A44	29.00000	11.08483	12.51323
198	435	A45	29.00000	12.37731	12.51323
272	413	A46	35.00000	17.13851	19.22065

Table C-6. Minimum noise, channels 5 and 1, no preprocessing.

Line	Pixel	Name	Pixel val	Local SNR	Global SNR
133	50	A1A	26.00000	15.37291	15.53756
133	51	A1B	21.00000	19.45158	20.11377
137	76	A2A	22.00000	19.01599	19.37149
137	77	A2B	21.00000	19.92917	20.11377
162	51	A3A	29.00000	14.42188	10.86345
163	50	A3B	29.00000	14.43850	10.86345
57	194	A4A	24.00000	18.06302	17.66436
58	195	A4B	21.00000	20.80436	20.11377
237	66	A5A	22.00000	20.91653	19.37149
237	67	A5B	26.00000	17.25636	15.53756
245	158	A6A	43.00000	19.88492	18.19705
246	158	A6B	44.00000	20.88132	19.04172
199	92	A7	32.00000	3.73474	0.02730
188	235	A8	43.00000	18.16886	18.19705
259	119	A9	25.00000	18.48232	16.66589
298	90	A10	19.00000	20.87400	21.43145
322	97	A11	19.00000	21.89744	21.43145
360	107	A12	24.00000	19.03107	17.66436
403	7	A13	31.00000	12.51548	5.26339
382	32	A14	27.00000	17.24889	14.24045
417	32	A15	29.00000	12.97928	10.86345
404	40	A16	24.00000	17.95919	17.66436
474	8	A17	30.00000	11.37887	8.50713
506	149	A18	21.00000	12.13800	20.11377
508	171	A19	22.00000	12.33486	19.37149
475	140	A20	26.00000	17.67335	15.53756
463	160	A21	26.00000	17.84381	15.53756
454	182	A22	29.00000	12.18016	10.86345
441	203	A23	25.00000	16.73686	16.66589
432	204	A24	23.00000	18.33480	18.55980
428	211	A25	31.00000	5.96738	5.26339
393	155	A26	25.00000	10.94818	16.66589
377	216	A27	30.00000	11.26104	8.50713
346	250	A28	28.00000	15.75177	12.71504
285	207	A29	22.00000	19.56598	19.37149
262	192	A30	27.00000	14.00073	14.24045
418	280	A31	30.00000	4.86304	8.50713
420	311	A32	21.00000	18.10599	20.11377
440	302	A33	20.00000	17.94036	20.79757
478	256	A34	21.00000	18.40151	20.11377
454	392	A35	23.00000	20.30154	18.55980
492	395	A36	24.00000	18.75406	17.66436
489	401	A37	26.00000	16.66735	15.53756
478	498	A38	33.00000	-4.94467	-15.22566
9	330	A39	33.00000	-6.13650	-15.22566
98	291	A40	16.00000	21.42084	23.09532
118	303	A41	20.00000	17.43640	20.79757
170	341	A42	39.00000	11.42710	13.63571
121	373	A43	25.00000	6.53367	16.66589
183	434	A44	28.00000	11.07893	12.71504
198	435	A45	30.00000	8.10274	8.50713
272	413	A46	22.00000	17.04173	19.37149

Table C-7. Minimum noise, channels 1 and 5, preprocessed.

Line	Pixel	Name	Pixel val	Local SNR	Global SNR
133	50	A1A	50.00000	16.02261	17.45886
133	51	A1B	61.00000	20.32410	22.11472
137	76	A2A	53.00000	17.98388	18.99471
137	77	A2B	54.00000	18.65380	19.45172
162	51	A3A	46.00000	16.14147	14.86821
163	50	A3B	45.00000	15.36251	14.07879
57	194	A4A	50.00000	17.03802	17.45886
58	195	A4B	59.00000	21.14482	21.43340
237	66	A5A	61.00000	21.17553	22.11472
237	67	A5B	51.00000	17.15791	18.00155
245	158	A6A	18.00000	18.52890	17.99056
246	158	A6B	14.00000	20.52005	19.87703
199	92	A7	43.00000	12.18818	12.24541
188	235	A8	12.00000	18.76796	20.68600
259	119	A9	54.00000	19.91112	19.45172
298	90	A10	65.00000	20.31334	23.33534
322	97	A11	69.00000	21.86564	24.40539
360	107	A12	61.00000	21.22831	22.11472
403	7	A13	46.00000	14.78591	14.86821
382	32	A14	53.00000	18.19684	18.99471
417	32	A15	47.00000	12.96003	15.59183
404	40	A16	59.00000	18.03839	21.43340
474	8	A17	48.00000	14.54017	16.25976
506	149	A18	72.00000	18.69081	25.12942
508	171	A19	73.00000	19.77211	25.35794
475	140	A20	55.00000	19.66318	19.88588
463	160	A21	54.00000	18.93725	19.45172
454	182	A22	45.00000	12.47961	14.07879
441	203	A23	54.00000	16.68949	19.45172
432	204	A24	56.00000	17.07970	20.29936
428	211	A25	45.00000	10.78576	14.07879
393	155	A26	34.00000	-17.51077	-12.55745
377	216	A27	46.00000	15.04015	14.86821
346	250	A28	48.00000	17.13220	16.25976
285	207	A29	57.00000	18.86016	20.69405
262	192	A30	50.00000	15.70276	17.45886
418	280	A31	55.00000	14.27230	19.88588
420	311	A32	64.00000	19.32911	23.04589
440	302	A33	60.00000	17.29492	21.78074
478	256	A34	67.00000	20.04259	23.88683
454	392	A35	54.00000	19.06127	19.45172
492	395	A36	53.00000	17.69260	18.99471
489	401	A37	53.00000	17.51050	18.99471
478	498	A38	36.00000	-7.06374	-2.77157
9	330	A39	33.00000	-3.62896	-2.89245
98	291	A40	71.00000	22.43418	24.89472
118	303	A41	61.00000	18.32983	22.11472
170	341	A42	29.00000	4.14606	8.43713
121	373	A43	51.00000	9.79541	18.00155
183	434	A44	52.00000	16.09825	18.51232
198	435	A45	47.00000	13.81605	15.59183
272	413	A46	62.00000	18.78494	22.43633

Table C-8. Minimum noise, channels 5 and 1; preprocessed.

Line	Pixel	Name	Pixel val	Local SNR	Global SNR
133	50	A1A	29.00000	16.65678	18.38717
133	51	A1B	18.00000	20.54447	22.62886
137	76	A2A	26.00000	18.38977	19.76359
137	77	A2B	24.00000	19.40650	20.57326
162	51	A3A	34.00000	16.57766	15.45886
163	50	A3B	35.00000	15.86384	14.73286
57	194	A4A	30.00000	17.49289	17.87522
58	195	A4B	21.00000	21.42741	21.66173
237	66	A5A	18.00000	21.59146	22.62886
237	67	A5B	29.00000	17.42889	18.38717
245	158	A6A	63.00000	18.54029	17.90567
246	158	A6B	67.00000	20.52421	19.78810
199	92	A7	39.00000	11.26801	11.00844
188	235	A8	70.00000	19.06575	20.97282
259	119	A9	25.00000	20.32002	20.17785
298	90	A10	13.00000	20.65070	24.03417
322	97	A11	8.00000	22.38051	25.24347
360	107	A12	18.00000	21.39224	22.62886
403	7	A13	36.00000	13.70128	13.94061
382	32	A14	27.00000	18.29110	19.32858
417	32	A15	31.00000	14.37622	17.33119
404	40	A16	20.00000	18.34177	21.99621
474	8	A17	35.00000	12.86880	14.73286
506	149	A18	6.00000	19.11337	25.68367
508	171	A19	5.00000	20.10514	25.89568
475	140	A20	24.00000	20.14408	20.57326
463	160	A21	30.00000	17.39120	17.87522
454	182	A22	38.00000	10.66431	12.09955
441	203	A23	26.00000	17.12608	19.76359
432	204	A24	27.00000	16.22676	19.32858
428	211	A25	35.00000	11.54768	14.73286
393	155	A26	46.00000	-18.14977	-12.99738
377	216	A27	38.00000	12.32922	12.09955
346	250	A28	34.00000	16.22068	15.45886
285	207	A29	23.00000	18.73442	20.95144
262	192	A30	29.00000	16.53267	18.38717
418	280	A31	25.00000	14.57386	20.17785
420	311	A32	14.00000	19.79203	23.77071
440	302	A33	19.00000	17.73445	22.31829
478	256	A34	14.00000	19.86955	23.77071
454	392	A35	28.00000	19.19569	18.87062
492	395	A36	25.00000	19.18844	20.17785
489	401	A37	29.00000	17.26612	18.38717
478	498	A38	45.00000	-7.98254	-3.10651
9	330	A39	48.00000	-2.61790	-2.77151
98	291	A40	6.00000	22.83877	25.68367
118	303	A41	18.00000	18.44745	22.62886
170	341	A42	53.00000	5.64155	9.83761
121	373	A43	28.00000	10.53008	18.87062
183	434	A44	29.00000	15.94966	18.38717
198	435	A45	34.00000	13.67963	15.45886
272	413	A46	16.00000	19.41018	23.21853

Table C-9. Simple difference, channels 1 and 5, no preprocessing.

Line	Pixel	Name	Pixel val	Local SNR	Global SNR
133	50	A1A	32.00000	15.37109	15.54239
133	51	A1B	37.00000	19.45013	20.12693
137	76	A2A	36.00000	19.01599	19.38358
137	77	A2B	37.00000	19.92917	20.12693
162	51	A3A	29.00000	14.42188	10.85377
163	50	A3B	29.00000	14.43850	10.85377
57	194	A4A	34.00000	18.02621	17.67362
58	195	A4B	37.00000	20.73136	20.12693
237	66	A5A	36.00000	20.93970	19.38358
237	67	A5B	32.00000	17.23372	15.54239
245	158	A6A	14.00000	20.61410	19.08043
246	158	A6B	14.00000	20.78595	19.08043
199	92	A7	27.00000	8.51883	5.22204
188	235	A8	14.00000	18.94280	19.08043
259	119	A9	33.00000	18.48232	16.67321
298	90	A10	39.00000	20.87125	21.44631
322	97	A11	39.00000	21.84081	21.44631
360	107	A12	34.00000	19.06333	17.67362
403	7	A13	28.00000	14.38342	8.48656
382	32	A14	31.00000	17.30161	14.24201
417	32	A15	29.00000	12.96906	10.85377
404	40	A16	34.00000	17.92350	17.67362
474	8	A17	29.00000	12.86577	10.85377
506	149	A18	37.00000	12.10310	20.12693
508	171	A19	36.00000	12.24652	19.38358
475	140	A20	32.00000	17.78824	15.54239
463	160	A21	33.00000	18.81455	16.67321
454	182	A22	29.00000	12.33164	10.85377
441	203	A23	33.00000	16.56220	16.67321
432	204	A24	36.00000	18.94770	19.38358
428	211	A25	27.00000	5.77204	5.22204
393	155	A26	33.00000	10.95981	16.67321
377	216	A27	29.00000	13.17847	10.85377
346	250	A28	31.00000	17.19125	14.24201
285	207	A29	36.00000	19.57293	19.38358
262	192	A30	31.00000	13.99416	14.24201
418	280	A31	28.00000	4.90595	8.48656
420	311	A32	37.00000	18.13732	20.12693
440	302	A33	38.00000	18.07336	20.81165
478	256	A34	37.00000	18.55390	20.12693
454	392	A35	36.00000	20.76050	19.38358
492	395	A36	34.00000	18.42007	17.67362
489	401	A37	33.00000	17.45537	16.67321
478	498	A38	25.00000	-5.06116	-15.93137
9	330	A39	26.00000	-7.69420	-6.06946
98	291	A40	42.00000	21.91499	23.11197
118	303	A41	38.00000	17.77667	20.81165
170	341	A42	20.00000	9.74230	12.04488
121	373	A43	33.00000	6.52587	16.67321
183	434	A44	29.00000	9.60797	10.85377
198	435	A45	29.00000	10.69957	10.85377
272	413	A46	36.00000	17.04091	19.38358

Table C-10. Simple difference, channels 1 and 5, preprocessed.

Line	Pixel	Name	Pixel val	Local SNR	Global SNR
133	50	A1A	51.00000	16.22560	17.78472
133	51	A1B	62.00000	20.34799	22.27235
137	76	A2A	54.00000	18.05914	19.25525
137	77	A2B	56.00000	19.12528	20.11330
162	51	A3A	47.00000	16.62221	15.33251
163	50	A3B	45.00000	15.06612	13.78596
57	194	A4A	51.00000	17.40089	17.78472
58	195	A4B	60.00000	21.38097	21.61055
237	66	A5A	62.00000	21.31522	22.27235
237	67	A5B	52.00000	17.43573	18.30306
245	158	A6A	18.00000	18.63743	18.03507
246	158	A6B	14.00000	20.60875	19.89636
199	92	A7	43.00000	12.04107	11.90307
188	235	A8	12.00000	18.79436	20.69607
259	119	A9	55.00000	20.02104	19.69487
298	90	A10	67.00000	20.52220	23.73501
322	97	A11	72.00000	22.21943	24.98650
360	107	A12	63.00000	21.50818	22.58525
403	7	A13	46.00000	14.45364	14.59361
382	32	A14	54.00000	18.38504	19.25525
417	32	A15	49.00000	13.84769	16.64487
404	40	A16	61.00000	18.42846	21.94775
474	8	A17	47.00000	13.54165	15.33251
506	149	A18	74.00000	18.89304	25.44062
508	171	A19	75.00000	19.92278	25.65907
475	140	A20	56.00000	19.75880	20.11330
463	160	A21	53.00000	18.32460	18.79220
454	182	A22	44.00000	11.43797	12.89544
441	203	A23	55.00000	17.02972	19.69487
432	204	A24	56.00000	16.97133	20.11330
428	211	A25	46.00000	11.35706	14.59361
393	155	A26	35.00000	-23.28901	-18.06498
377	216	A27	45.00000	14.07800	13.78596
346	250	A28	48.00000	16.87482	16.01345
285	207	A29	58.00000	18.84143	20.89415
262	192	A30	51.00000	15.99623	17.78472
418	280	A31	56.00000	14.47204	20.11330
420	311	A32	66.00000	19.64910	23.46152
440	302	A33	62.00000	17.69850	22.27235
478	256	A34	68.00000	20.10480	24.00015
454	392	A35	54.00000	19.24547	19.25525
492	395	A36	55.00000	18.56292	19.69487
489	401	A37	53.00000	17.47102	18.79220
478	498	A38	36.00000	-8.99934	-4.41606
9	330	A39	33.00000	-1.87627	-1.63907
98	291	A40	74.00000	22.77999	25.44062
118	303	A41	62.00000	18.26562	22.27235
170	341	A42	29.00000	4.44822	8.73597
121	373	A43	53.00000	10.47408	18.79220
183	434	A44	52.00000	15.91463	18.30306
198	435	A45	47.00000	13.53255	15.33251
272	413	A46	63.00000	18.88253	22.58525

APPENDIX D: DETAILS OF NUMERIC RESULTS, HUNTSVILLE DATA SET

The TIMS Huntsville data set was processed to confirm results achieved by using the TIMS Adelaide data set. The TIMS Adelaide data set was processed to compare the results to the spatial difference model developed by L. E. Hoff.

The first step in this processing was to determine which two of the six TIMS bands met the criterion of high correlation between the bands. A routine was run on the raw data that produces a correlation coefficient matrix, as shown in figure D-1. It was also desirable for this processing that the bands be widely separated, which tends to preserve target coloring. Bands 1 and 4, with a correlation coefficient of 0.9015, were chosen.

$$\begin{pmatrix} 1.000*10^{0} & 9.750*10^{-1} & 9.376*10^{-1} & 9.015*10^{-1} & 8.300*10^{-1} & 7.647*10^{-1} \\ 9.750*10^{-1} & 1.000*10^{0} & 9.374*10^{-1} & 8.827*10^{-1} & 7.938*10^{-1} & 7.315*10^{-1} \\ 9.376*10^{-1} & 9.374*10^{-1} & 1.000*10^{0} & 8.034*10^{-1} & 7.314*10^{-1} & 5.921*10^{-1} \\ 9.015*10^{-1} & 8.827*10^{-1} & 8.034*10^{-1} & 1.000*10^{0} & 9.625*10^{-1} & 8.958*10^{-1} \\ 8.300*10^{-1} & 7.938*10^{-1} & 7.314*10^{-1} & 9.625*10^{-1} & 1.000*10^{0} & 9.084*10^{-1} \\ 7.647*10^{-1} & 7.315*10^{-1} & 5.921*10^{-1} & 8.958*10^{-1} & 9.084*10^{-1} & 1.000*10^{0} \end{pmatrix}$$

Figure D-1. Correlation coefficient matrix.

The second step in the processing was to window the area of interest. An area that was 256 × 256 in size was chosen. From this area, 22 target pixels were chosen for this processing run. Figure D-2 identifies the target pixels by line and column.

Line	Pixel	Pixel Name	Line	Pixel	Pixel Name
160	114	TA1	216	189	R2
159	113	TA2	216	190	R3
159	114	TA3	216	191	R4
104	181	TC1	216	192	R5
104	182	TC2	216	193	R6
103	180	TC3	217	188	R7
103	181	TC4	217	189	R8
56	148	S1	217	190	R9
56	149	S2	217	191	R10
56	150	S3	217	192	R11
216	188	R1	217	193	R12

Figure D-2. Huntsville target pixels.

Three different preprocessing methods were used on this data set. The first case did a global normalization on the image, which took the mean and variance of the entire 256 × 256 image to

compute pixel values. The second case did a line-by-line normalization on the data, which entailed taking the mean and variance of each line to determine the pixel values and then doing a global normalization on the data. The third case did a line-by-line normalization on the data, followed by a high-pass 5 $\times$ 5 filter. As a last step, the data set was globally normalized. The final output of the preprocessing phase of this image processing consisted of six files, three each of band 1 and band 4, globally normalized, line-by-line normalized, and filtered.

For each case, and at each target pixel, the band with the largest signal-to-noise (SNR) was determined and the data set was entered into a database (see tables D-1, D-2, and D-3). The pixel values that determined the color ratio for comparison purposes were also entered at this time.

Upon completion of the preprocessing steps, three weighted-difference algorithms were applied to each set (band 1 and band 4) of data. Each of these algorithms used a different weighting factor; one maximized the output SNR, Max_SNR; one minimized the noise, Min_Noise; and one used a weighting factor of 1, Sim_Diff. The Min_Noise algorithm was applied twice to each data set. One run applied band 1 to band 4; the second run applied band 4 to band 1. The SNR for each target pixel from each output image was then measured and entered into the database with the input band's SNRs (tables D-1 through D-3). The dB gain was then computed from the input and output SNR information and entered into the database. The data provided the necessary information for comparing the spatial-difference model to the Huntsville data.

Table D-1. Huntsville normalized (entire image only) channels 1 and 4 target data.

NAME	LINE	PIXEL	> SNR IN (dB)	BAND	PIXEL VALUE FM>SNRIN	FM<SNRIN	COLOR RATIO	SNR OUT (in dB) MAX SNR	MIN 1-4	MIN 4-1	SIMP SNR	dB GAIN MAX	MIN1-4	MIN4-1	SIMPLE
TA1	160	114	12.48913	4	-4.21172	-1.04058	0.247068	17.13642	15.31216	17.04448	16.47454	4.65	2.82	-12.49	3.985
TA2	159	113	15.5718	1	-6.00608	-4.7039	0.78319	15.78467	11.97502	2.58105	8.74364	0.21	-3.60	-15.57	-6.83
TA3	159	114	11.71388	1	-3.85208	-3.02248	0.784636	11.921	8.08058	-1.39892	4.82762	0.21	-3.63	-11.71	-6.89
TC1	104	181	15.47961	4	-5.94269	-4.79364	0.806645	15.60826	0.25886	11.27034	7.65699	0.13	-15.22	-15.48	-7.82
TC2	104	182	6.69146	4	-2.16061	-1.37092	0.634506	7.82388	1.43213	6.21113	4.39935	1.13	-5.26	-6.69	-2.29
TC3	103	180	11.33738	4	-3.68869	-3.4864	0.945159	11.40618	-6.63335	2.22339	-7.43017	0.07	-17.97	5.71	-18.8
TC4	103	181	11.37194	1	-3.70338	-3.53884	0.95557	11.46711	1.74773	-5.17338	-9.22455	0.10	-9.62	-8.79	-20.6
S1	56	148	24.70405	4	-17.1872	-13.8484	0.805736	24.83558	9.58123	20.51933	16.92216	0.13	-15.12	-26.10	-7.78
S2	56	149	27.10585	1	-22.6618	-19.9866	0.881952	27.10639	20.57466	-12.5445	14.99729	0.00	-6.53	-15.84	-12.1
S3	56	150	-0.79702	1	0.91233	0.43432	0.476056	1.73072	1.14263	-1.82273	0.03898	2.53	1.94	7.01	0.836
R1	216	188	12.41479	1	-4.17581	-2.39727	0.574085	14.05144	12.93829	9.02037	11.45148	1.64	0.52	-10.19	-0.96
R2	216	189	13.52238	1	-4.74374	-2.44946	0.516356	15.67691	14.90747	11.59956	13.66314	2.15	1.39	-18.70	0.141
R3	216	190	12.15045	1	-4.05064	-1.95579	0.482835	14.61497	13.99922	10.98011	12.87328	2.46	1.85	8.37	0.723
R4	216	191	13.0912	1	-4.514	-2.00297	0.443724	15.92167	15.45141	12.72358	14.44724	2.83	2.36	-25.64	1.356
R5	216	192	12.63723	1	-4.28413	-1.88302	0.439534	15.50702	15.0505	12.35139	14.05846	2.87	2.41	-14.46	1.421
R6	216	193	5.82212	1	-1.95482	-0.87993	0.450134	8.59245	8.10058	5.32797	7.07753	2.77	2.28	3.20	1.255
R7	217	188	-2.41604	1	-0.75718	-0.11145	0.147191	3.09896	3.07242	1.66698	2.65119	5.52	5.49	14.02	5.067
R8	217	189	8.34214	1	-2.61281	-1.02406	0.391938	11.6589	11.33631	8.93471	10.47135	3.32	2.99	2.64	2.129
R9	217	190	7.33728	1	-2.32737	-0.92145	0.395919	10.6167	10.28431	7.85967	9.40942	3.28	2.95	5.39	2.072
R10	217	191	8.93031	1	-2.79587	-1.25211	0.447843	11.72214	11.23809	8.48161	10.22184	2.79	2.31	3.42	1.292
R11	217	192	9.16872	1	-2.87367	-1.08695	0.378245	12.61373	12.32307	9.9984	11.49137	3.45	3.15	-3.84	2.323
R12	217	193	-8.77609	1	-0.36408	-0.12632	0.346957	-5.0394	-5.26642	-7.42771	-6.02692	3.74	3.51	10.44	2.749

Table D-2. Huntsville normalized (line by line, then entire image) channels 1 and 4 target data.

			> SNR IN		PIXEL VALUE		COLOR	SNR OUT (in dB)				dB GAIN			
NAME	LINE	PIXEL	(dB)	BAND	FM>SNRIN	FM<SNRIN	RATIO	MAX SNR	MIN 1-4	MIN 4-1	SIMP SNR	MAX	MIN1-4	MIN4-1	SIMPLE
TA1	160	114	-3.24351	1	0.68837	-0.6198	-0.90039	9.62506	9.43915	9.39456	9.62436	12.87	12.68	3.24	12.87
TA2	159	113	2.11047	1	-1.27504	-0.80193	0.628945	3.67506	2.27285	-1.5179	0.79012	1.56	0.16	-2.11	-1.32
TA3	159	114	-8.38686	1	-0.38706	0.01489	-0.03847	-0.58452	-0.58572	-1.37233	-0.76265	7.80	7.80	8.39	7.624
TC1	104	181	6.90206	4	-2.21362	-1.50559	0.680148	8.00309	1.50416	6.07156	4.29215	1.10	-5.40	-6.90	-2.61
TC2	104	182	-5.15917	4	-0.55213	0.02666	-0.04829	2.71333	1.93935	2.71154	2.54149	7.87	7.10	5.16	7.701
TC3	103	180	1.57368	4	-1.19863	-0.84642	0.706156	2.45889	-4.88357	0.19156	-1.77301	0.89	-6.46	7.82	-3.35
TC4	103	181	1.57368	4	-1.19863	-0.99078	0.826594	1.72764	-12.8544	-2.95087	-6.35408	0.15	-14.43	-3.09	-7.93
S1	56	148	18.12423	4	-8.05772	-6.30825	0.782883	18.48333	7.4786	14.87541	12.14916	0.36	-10.65	-19.50	-5.98
S2	56	149	20.16325	1	-10.1897	-9.20074	0.902945	20.16368	12.82955	-20.8396	7.1946	0.00	-7.33	-14.09	-13
S3	56	150	-7.38716	1	0.42721	-0.24706	-0.57831	3.88291	3.77306	3.5459	3.8677	11.27	11.16	10.10	11.25
R1	216	188	2.70545	1	-1.36544	-0.24763	0.181355	8.67977	8.64351	7.41479	8.325832	5.97	5.94	-2.51	5.62
R2	216	189	5.12397	1	-1.80384	-0.36503	0.202363	10.90911	10.86176	9.057806	10.45107	5.79	5.74	-8.07	5.327
R3	216	190	4.39016	1	-1.6577	-0.24763	0.149382	10.64763	10.62449	9.4742	10.27584	6.26	6.23	10.49	5.886
R4	216	191	5.12397	1	-1.80384	-0.24763	0.137279	11.48686	11.46784	10.34571	11.13235	6.36	6.34	-25.96	6.008
R5	216	192	3.58859	1	-1.51157	-0.13024	0.086162	10.38743	10.38055	9.36907	10.09699	6.80	6.79	-0.04	6.508
R6	216	193	-9.30675	1	-0.3425	0.33935	-0.9908	3.96495	3.75934	3.75538	3.96483	13.27	13.07	16.72	13.27
R7	217	188	-4.14879	4	0.62024	0.13607	0.219383	1.48093	0.09299	1.42333	0.99108	5.63	4.24	13.21	5.14
R8	217	189	-1.64255	1	-0.8277	0.17391	-0.21011	7.39467	7.37062	6.81556	7.30499	9.04	9.01	11.12	8.948
R9	217	190	-1.64255	1	-0.8277	0.17391	-0.21011	7.39467	7.37062	6.81566	7.30499	9.04	9.01	11.99	8.948
R10	217	191	-0.30604	1	-0.96538	0.06233	-0.06457	7.68964	7.68661	6.93921	7.52841	8.00	7.99	9.68	7.834
R11	217	192	-1.64255	1	-0.8277	0.17391	-0.21011	7.39467	7.37062	6.81556	7.30499	9.04	9.01	5.40	8.948
R12	217	193	-4.14879	4	0.62024	0.41143	0.66334	-2.9006	-8.92499	-4.64059	-6.31379	1.25	-4.78	5.57	-2.17

Table D-3. Huntsville normalized (line by line/high-pass filter/then renormalized) channels 1 and 4 target data.

NAME	LINE	PIXEL	> SNR IN (dB)	BAND	PIXEL VALUE FM>SNRIN	FM<SNRIN	COLOR RATIO	SNR OUT (in dB) MAX SNR	MIN 1-4	MIN 4-1	SIMP SNR	dB GAIN MAX	MIN1-4	MIN4-1	SIMPLE
TA1	160	114	-0.92928	4	-0.89854	0.21357	-0.23769	9.62506	9.43914	9.39458	9.62436	10.55	10.37	0.93	10.55
TA2	159	113	3.25467	1	-1.45458	-1.02086	0.701825	3.67506	2.27289	-1.5178	0.79019	0.42	-0.98	-3.25	-2.46
TA3	159	114	-2.38934	1	-0.75952	-0.28695	0.377804	-0.58452	-0.58572	-1.3723	-0.76264	1.80	1.80	2.39	1.627
TC1	104	181	7.91936	4	-2.48869	-1.73261	0.696194	8.00308	1.50403	6.0715	4.29207	0.08	-6.42	-7.92	-3.63
TC2	104	182	-2.20032	4	-0.77622	-0.20347	0.262129	2.71333	1.93932	2.71154	2.54148	4.91	4.14	2.20	4.742
TC3	103	180	2.8466	4	-1.38782	-0.89853	0.64744	2.45889	-4.88372	0.19151	-1.77311	-0.39	-7.73	6.55	-4.62
TC4	103	181	2.8466	4	-1.38782	-1.03754	0.747604	1.72762	-12.8547	-2.95097	-6.35425	-1.12	-15.70	-4.36	-5.2
S1	56	148	20.27111	4	-10.3171	-7.71018	0.747318	18.48333	7.47836	14.87533	12.14903	-1.79	-12.79	-21.64	-8.12
S2	56	149	21.89395	1	-12.4366	-11.785	0.947601	20.1637	12.8297	-20.8318	7.19491	-1.73	-9.06	-15.82	-14.7
S3	56	150	-6.16785	1	0.4916	-0.28695	-0.58371	3.8829	3.77305	3.54593	3.8677	10.05	9.94	8.88	10.04
R1	216	188	-0.92944	1	-0.89853	-0.04231	0.047088	8.67977	8.64351	7.41483	8.25835	9.61	9.57	1.12	9.188
R2	216	189	2.38218	1	-1.31557	-0.16463	0.12514	10.9091	10.86176	9.57811	10.45109	8.53	8.48	-5.33	8.069
R3	216	190	1.41216	1	-1.17656	-0.04231	0.035961	10.64763	10.62449	9.47423	10.27586	9.24	9.21	13.46	8.864
R4	216	191	2.38218	1	-1.31557	-0.04231	0.032161	11.48645	11.46785	10.34575	11.13237	9.10	9.09	-23.21	8.75
R5	216	192	0.32003	1	-1.03754	0.08001	-0.07712	10.38743	10.38055	9.36911	10.09701	10.07	10.06	3.23	9.777
R6	216	193	-4.89343	4	0.56929	0.07456	0.13097	3.96495	3.75933	3.7554	3.96483	8.86	8.65	12.31	8.858
R7	217	188	-1.78836	4	0.81393	0.4916	0.603983	1.48093	0.09295	1.42332	0.99105	3.27	1.88	11.37	2.779
R8	217	189	-6.34833	1	-0.48149	0.32465	-0.67426	7.39467	7.37062	6.81559	7.305	13.74	13.72	15.82	13.65
R9	217	190	-6.34833	1	-0.48149	0.32465	-0.67426	7.39467	7.37062	6.81559	7.305	13.74	13.72	16.69	13.65
R10	217	191	-4.1452	1	-0.6205	0.20233	-0.32608	7.68964	7.68661	6.93924	7.52843	11.83	11.83	13.51	11.67
R11	217	192	-6.34833	1	-0.48149	0.32465	-0.67426	7.39467	7.37062	6.81559	7.305	13.74	13.72	10.10	13.65
R12	217	193	-1.78836	4	0.81393	0.76963	0.945573	-2.9006	-8.92511	-4.64064	-6.31387	-1.11	-7.14	3.21	-4.53

REPORT DOCUMENTATION PAGE

Form Approved
OMB No. 0704-0188

1. AGENCY USE ONLY *(Leave blank)*	2. REPORT DATE	3. REPORT TYPE AND DATES COVERED
	December 1990	Final: Oct 1989 – Dec 1990

4. TITLE AND SUBTITLE

DETECTION OF TARGETS IN TERRAIN CLUTTER BY USING MULTISPECTRAL INFRARED IMAGE PROCESSING

5. FUNDING NUMBERS

Program Element: 0603226E
Project No.: SX34
Accession No.: DN388563

6. AUTHOR(S)

L. E. Hoff, J. R. Evans, and L. E. Bunney

7. PERFORMING ORGANIZATION NAME(S) AND ADDRESS(ES)

Naval Ocean Systems Center (Code 765)
San Diego, CA 92152–5000

8. PERFORMING ORGANIZATION REPORT NUMBER

NOSC TR 1404

9. SPONSORING/MONITORING AGENCY NAME(S) AND ADDRESS(ES)

Defense Advanced Research Project Agency (Code AVSTO)
1400 Wilson Boulevard
Arlington, VA 22209

10. SPONSORING/MONITORING AGENCY REPORT NUMBER

11. SUPPLEMENTARY NOTES

12a. DISTRIBUTION/AVAILABILITY STATEMENT

Approved for public release; distribution is unlimited.

12b. DISTRIBUTION CODE

13. ABSTRACT *(Maximum 200 words)*

A weighted-difference signal-processing algorithm for detecting ground targets by using dual-band IR data was investigated. Three variations of the algorithm were evaluated: (1) simple difference; (2) minimum noise; and (3) maximum SNR. The theoretical performance was compared to measured performance for two scenes collected by the NASA TIMS sensor over a rural area near Adelaide, Australia, and over a wooded area near the Redstone Arsenal. The theoretical and measured results agreed extremely well. For a given correlation coefficient and color ratio, the amount of signal-to-noise ratio gain can be predicted. However, target input SNRs and color ratios can vary considerably. For the targets and scenes evaluated here, the typical gains achieved ranged from a few dB loss (targets without color) to a maximum of approximately 20 dB.

14. SUBJECT TERMS

IR surveillance, wide-area surveillance, clutter, ground targets, camouflage, weighted-difference algorithm, dual-band IR, signal-to-noise ratios (SNRs), color ratios

15. NUMBER OF PAGES: 55

16. PRICE CODE

17. SECURITY CLASSIFICATION OF REPORT	18. SECURITY CLASSIFICATION OF THIS PAGE	19. SECURITY CLASSIFICATION OF ABSTRACT	20. LIMITATION OF ABSTRACT
UNCLASSIFIED	UNCLASSIFIED	UNCLASSIFIED	SAME AS REPORT

21a. NAME OF RESPONSIBLE INDIVIDUAL	21b. TELEPHONE *(Include Area Code)*	21c. OFFICE SYMBOL
L.E. Hoff	(619)553-6186	Code 7602

INITIAL DISTRIBUTION

Code 0012	Patent Counsel	(1)
Code 014	G. Dillard	(1)
Code 0144	R. November	(1)
Code 705	V. Pusateri	(1)
Code 73	J. Roese	(1)
Code 731	C. Goodhart	(1)
Code 732	C. Persons	(1)
Code 7502	B. Hunt	(1)
Code 754	D. Frost	(1)
Code 76	F. Tirpak	(1)
Code 7601	C. Bass	(1)
Code 7601	K. Bromley	(1)
Code 7601	J. Zeidler	(1)
Code 7602	L. Hoff	(25)
Code 761	R. Bocker	(1)
Code 761	J. Loughlin	(1)
Code 761	J. Symanski	(1)
Code 764	S. Darensburg	(1)
Code 765	L. Bunney	(1)
Code 765	R. Carlson	(1)
Code 765	J. Evans	(1)
Code 765	R. Patterson	(1)
Code 765	D. Williams	(1)
Code 952B	J. Puleo	(1)
Code 961	Archive/Stock	(6)
Code 964B	Library	(3)

Defense Technical Information Center
Alexandria, VA 22304-6145 (4)

NOSC Liaison Office
Washington, DC 20363-5100 (1)

Naval Research Laboratory
Washington, DC 20375-5000 (1)

Space & Naval Warfare Systems Command
Washington, DC 20363-5100 (1)

Colorado State University
Fort Collins, CO 80523 (1)

Environmental Research Institute of Michigan
Ann Arbor, MI 48107-8618 (1)

General Electric
Schenectady, NY 12301 (1)

Lawrence Livermoore Laboratory
Livermoore, CA 94550 (5)

Lockheed Missile & Space Company
Palo Alto, CA 94304-1191 (2)

Defense Advanced Research Project Agency
Arlington, VA 22209-2308 (1)

Center for Naval Analyses
Alexandria, VA 22302-0268 (1)

Office of Naval Technology
Arlington, VA 22217-5000 (2)

U.S. Army Missile Command
Redstone Arsenal, AL 35898-5244 (2)

ADS
Mountain View, CA 94043 (1)

General Dynamics
Rancho Cucamonga, CA 91730 (1)

Itek Optical Systems
Arlington, VA 22209-1973 (1)

Litton Data Systems
Van Nuys, CA 91409 (1)

Loral Fairchild Systems
Syosset, NY 11791 (1)

MDTI
San Diego, CA 92198 (1)

Technical Research Associates
Camarillo, CA 93010 (1)

SPIE
Bellingham, WA 98227-0010 (1)

TITAN Systems, Inc.
San Diego, CA 92121 (2)